Collapse Performance of Low-Ductility Chevron Braced Steel Frames in Moderate Seismic Regions

ERIC M. HINES, MARY E. APPEL and PETER J. CHEEVER

Prior to 1978, seismic design practice in the United States distinguished moderate seismic regions from high seismic regions through the application of lower design acceleration levels (SEAOC, 1960; Rojahn, 1995). In 1978 the Applied Technology Council's document ATC-3-06 proposed further differentiation between moderate and high seismic regions by regulating structural systems and detailing requirements according to Seismic Design Category (SDC) (ATC, 1978). Since the publication of ATC-3-06, detailing requirements have grown more numerous and stringent for buildings in high seismic regions (SDC D or higher); however, they have not influenced building design in low and moderate seismic regions (SDC C or lower) as heavily. Thus, it has generally been accepted that buildings in low and moderate seismic regions may be designed both for lower maximum considered earthquake (MCE) forces and less ductility than their counterparts in high seismic regions. Current model codes adhere to this philosophy by assigning different height limits to recognized structural systems in each SDC (ICC, 2006; ASCE, 2005). Each recognized system is assigned a response modification factor (R-factor), which applies to all SDCs.

Language in the 1992 AISC *Seismic Provisions* (AISC, 1992) clearly exempted most buildings in SDC A, B, and C from seismic detailing requirements. This exemption generated the unintended consequence that some engineers designed buildings in low and moderate seismic regions with high R-factors, but without providing appropriate detailing. The 1997 AISC *Seismic Provisions* clarified the intention of the SDC exemptions by specifying that "Systems designed and detailed to meet the requirements in the LRFD *Specification* but not the requirements of Part I" of the AISC *Seismic Provisions* should be designed with $R = 3$ (AISC, 1997a). Although this provision was originally intended to ensure a minimum design level for low-ductility systems, its ability to ensure collapse resistance similar to more ductile systems with higher R-factors has not been proven.

These historical circumstances motivate fundamental questions concerning seismic collapse behavior in moderate seismic regions.

1. How much ductility, how much strength, and how much reserve capacity are actually required for a building to survive an MCE event in a moderate seismic region?
2. In particular, can an inherently low-ductility system such as a concentric chevron braced steel frame be designed to survive moderate seismic demand with a high level of confidence?
3. Should such systems even be evaluated according to the concepts of ductility and capacity design?
4. How can we articulate a design philosophy for low-ductility systems in moderate seismic regions that aims to ensure safety against collapse while allowing engineers as much freedom as possible to design creatively and economically?

DESIGN PHILOSOPHY FOR MODERATE SEISMIC REGIONS

The absence of a clearly expressed low-ductility design philosophy for moderate seismic regions makes $R = 3$ appear to be an attractive option for the design of such systems. Further investigation reveals, however, that the literature is relatively silent on the adequacy of $R = 3$. In comparison to well-developed design philosophies such as ductility and capacity design, isolation, and supplemental damping, $R = 3$ offers little insight into structural behavior. A design philosophy for low-ductility systems in moderate seismic regions should encourage the development of structural systems according to well-established principles rather than prescriptive requirements. The analyses presented in this paper indicate that collapse vulnerability of an $R = 3$ system depends heavily on the capacity of its gravity framing to act as a reserve system. While conclusions regarding the safety of $R = 3$ in general remain beyond the scope of this paper, the studies presented herein yield some insight into reserve

---

Eric M. Hines is a professor of practice in the department of civil and environmental engineering, Tufts University, Medford, MA and an associate at LeMessurier Consultants, Cambridge, MA.

Mary E. Appel is a structural engineer at BSA Life Structures, Indianapolis.

Peter J. Cheever is an executive vice president at LeMessurier Consultants, Cambridge, MA.

system performance and other important characteristics of a low-ductility design philosophy. Such a philosophy should respond to the following observations:

1. Socioeconomic Impact
    a. Emphasize collapse prevention over economic loss (Luft and Simpson, 1979).
    b. Encourage owners, designers, and builders to develop creative approaches based on fundamental principles rather than follow prescriptive requirements that can, under certain circumstances, diminish rather than improve collapse performance.
2. Moderate Seismic Hazard
    a. Design event return periods are much longer than most high seismic regions (Bell and Lamontagne, 2002).
    b. Variability of possible earthquake magnitudes is higher than in most high seismic regions (Hines et al., 2009).
    c. Spectral acceleration values are generally higher than model codes in the low period range, and lower than model codes in the high period range (Leyendecker et al., 2000).
    d. Ground motions propagated through specific soil columns may produce response spectra that differ significantly from code prescribed values (Sorabella 2006, Appel 2008).
3. Low-Ductility Systems
    a. Member design of lateral force resisting systems (LFRSs) is often governed by wind forces and stiffness considerations.
    b. Potential variations in capacity of low-ductility systems are higher than variations in high-ductility systems.
    c. Taller buildings and moment frame structures often perform in the elastic range, even under ground motions whose spectral accelerations are more than twice the levels prescribed by model codes.
    d. Most buildings contain substantially more gravity framing than assigned directly to the primary LFRS. This gravity framing may be harnessed effectively and economically as a reserve system.
    e. Small amounts of ductility in the primary or reserve LFRS can increase collapse capacity substantially.

A design philosophy for low-ductility structures in moderate-seismic regions should draw not only on concepts of strength and ductility, but also elastic flexibility and reserve capacity to address the needs of individual structures. For instance, ordinary moment resisting frames (OMRFs) owe much of their robust behavior in moderate seismic regions to their elastic flexibility (Nelson, 2007). Collapse of low-ductility braced frames can be prevented by providing a flexible reserve system that is activated after brace fracture (Hines and Appel, 2007). Eccentric braced frames with longer links are well-suited to achieve moderate levels of ductility in the primary LFRS while allowing greater flexibility for coordination with architectural openings (Engelhardt and Popov, 1989). This paper focuses explicitly on low-ductility chevron braced steel frames and the consequences of enhancing their reserve capacity.

Results presented in this paper show that moment connecting a portion of the gravity framing for a building braced with chevron concentric-braced frames (CBFs) can increase collapse capacity substantially. Such reserve systems would require little to no increase in tonnage, and they would allow reductions in seismic story shear and overturning forces on the primary LFRS. This has the potential to reduce foundation costs. The reserve systems discussed in this paper provide stability primarily through their elastic flexibility and secondarily through their ductility. Overall, ductility demand on these reserve systems was observed to be very low, in the range of OMRFs. While moment connections do carry additional cost, this cost is typically lower than the cost of increased tonnage associated with moment frames as primary LFRS (as much as four times the tonnage of a CBF for equivalent stiffness). A hypothesis resulting from this study is that reserve systems for CBFs can be designed with OMRF connections and without consideration of either strong-column/weak-beam behavior or strong panel zone behavior. The force levels to which such reserve systems should be designed is beyond the scope of this introductory paper and should be the subject of future discussion.

The concept of a reserve system is well established in other contexts, such as higher ductility dual systems; the ASCE 7 general provision for redundancy, requiring stability of the lateral system even if an individual member is compromised; and the R = 3 concept itself. R = 3 clearly implies that the damaged primary system, gravity framing, façade and nonstructural components of a building possesses sufficient reserve capacity to prevent collapse under earthquake forces in an acceptable number of cases. The R = 3 criterion also implies that a response modification factor of 3 ensures the appropriate design force level for a given primary LFRS. Following a historical description of how this issue came to light in Boston, this study compares the effectiveness of primary LFRS strength versus reserve LFRS strength in improving collapse prevention performance.

HISTORICAL MOTIVATION FOR A CASE STUDY OF CHEVRON BRACED STEEL FRAMES IN BOSTON

The poor inelastic system performance of concentric chevron braced frames has been clearly demonstrated and discussed for decades, mostly in context of high seismic demands (Anderson, 1975; SEAONC, 1982; Shibata and Wakabayashi, 1983a, 1983b; Uang and Bertero, 1986; Khatib et al., 1988; Nakashima and Wakabayashi, 1992; Tremblay and Robert, 2000, 2001; Tremblay, 2001; Kim and Choi, 2004). From other structural design perspectives, however, chevron braced frames can be very attractive. Like most braced frames, they have a very high stiffness-to-weight ratio. They are generally symmetric, and they accommodate a variety of architectural openings. They are also statically determinate and assume gravity loads only from the floor which they support. These attractive attributes contrast starkly against their potentially poor seismic performance. Thus, they are interesting candidates for study in moderate seismic regions where the building community generally considers seismic concerns secondary to more conventional structural design concerns such as architectural coordination, stiffness and cost.

Historical aspects of the Massachusetts State Building Code make the Boston area particularly appropriate for this discussion of strength, ductility and reserve capacity. Since the 1970s, engineers, seismologists and public officials have worked to prepare Boston and other cities in Massachusetts for a destructive seismic event similar to the 1755 Cape Ann Earthquake. The success of these previous efforts, drawing heavily from the Seismic Design Decision Analysis project at MIT, was evidenced both in the creation and adoption of the "first seismic criteria developed specifically for a jurisdiction in the eastern United States" (Luft and Simpson, 1979) and in the Hazus Pilot Study conducted for Boston in the late 1990s (EQE, 1997). Luft and Simpson summarized the philosophical conclusions of this work as follows:

> The primary finding of these studies was that the probable maximum earthquake intensities for Massachusetts are as large as those for Zone 3 regions in California, but have much longer return periods. Because of the long return periods for destructive earthquakes, it was found that the cost to society of the earthquake-resistant design is considerably greater than the projected savings in damage and loss of life due to an earthquake. Nevertheless, the committee felt that society would insist on reasonable measures to mitigate the number of casualties from a major seismic event. It was therefore considered necessary to develop a set of criteria which would minimize the projected loss of life resulting from such an event, without causing construction costs to increase by an unacceptable amount. (p. 1)

These conclusions distinguished seismic design philosophy in Massachusetts from the contemporary SEAOC provisions for California by placing exclusive emphasis on protection against loss of life in an extreme event and ignoring the need to minimize the cost of damage in minor and moderate earthquakes (SEAOC, 1974).

Thirty years later, the philosophy described by Luft and Simpson remains valid for moderate seismic regions, where most building owners and occupants are unlikely to experience a major seismic event during their lifetime. In the meantime, however, this philosophy has experienced an interesting historical twist that deserves new attention. In the 1970s it was clear to the Massachusetts seismic committee that the least costly way to protect new building stock was to require design and detailing at an acceptable level of ductility. In light of seismic provisions issued since the 1990s to protect chevron braced frames in high seismic regions, however, it has become clear that the alternative $R = 3$ approach in SDC A, B and C results in chevron braced steel frames that are less expensive than the ordinary concentrically braced frame (OCBF) criteria listed in any edition of the AISC *Seismic Provisions*. This comparison came to light in Massachusetts because the sixth edition of the Massachusetts State Building Code required the 1992 AISC *Seismic Provisions* to apply to Seismic Design Category C (Massachusetts, 1996).

The contrast between $R = 3$ and the OCBF is demonstrated most clearly with the 2002 and 2005 AISC *Seismic Provisions* (AISC, 2002, 2005b). For instance, Section 14.2 of the 2002 *Provisions* required an overstrength factor of $\Omega = 2.0$ to be applied to all members and connections in an OCBF where $R = 5$, with the exception that brace connections should be designed for the expected tensile strength $R_yF_yA_g$ of the braces. The effective R-factor for such a frame was thus 2.5, less than 3.0. Coupling these higher forces with the more stringent connection requirements, the 2002 OCBF design was clearly more expensive than an $R = 3$ design.

In order to demonstrate this difference in detail, Gryniuk and Hines (2004) developed $R = 3$ and 2002 AISC OCBF designs for an eight-story student residence facility at the Wentworth Institute of Technology in Boston. These two designs were submitted to several fabricators for comparative pricing. Representative values from this study, demonstrating an 82% increase in lateral system cost, are reported in Table 1.

Similarly, simple calculations for a nine-story OCBF according to the 2005 AISC *Seismic Provisions* estimated a 70% increase in brace, beam and column tonnage over a comparable $R = 3$ design. The R-factor related to the 2005 OCBF was reduced from 5 to 3.25 in accordance with model code revisions, and the amplification of member forces was eliminated, making the OCBF member forces approximately 8% lower than the $R = 3$ design. The *b/t* requirement for hollow structural sections (HSS) and the capacity design requirements for columns and beams in a chevron configuration, however, kept the weight of the system significantly higher. Thus, it has become clear that, for the chevron CBF

Table 1. 2004 Cost Comparison of R = 3 and R = 5 Chevron Concentrically Braced Steel Frames According to the 2002 *AISC Seismic Provisions*

	Lateral System		
(1)	R = 3 (2)	OCBF 2002 (3)	OCBF %Inc (4)
Tons	73.38	154.75	110%
Material	$52,942	$115,803	119%
Freight	$8,219	$17,239	110%
Drafting	$53,029	$67,817	28%
Shop	$160,740	$354,780	121%
Erection	$120,100	$164,500	37%
Total	$395,030	$720,139	82%
Bms., Cols., Brcs.	248 pcs.	248 pcs.	
Draft Hrs.	920	1119	22%
Shop Hrs.	2679	5913	121%

configuration, an R = 3 design is more attractive than an OCBF with respect to construction cost and design effort in SDC A, B and C. This does not necessarily mean that an R = 3 chevron CBF design will safely conform to the seismic design philosophy for moderate seismic regions summarized by Luft and Simpson in 1979. Rather, it legitimates the question as to whether increased ductility is really the most economical approach to ensuring collapse resistance in moderate seismic regions.

DESIGN AND MODELING OF BRACED FRAME BUILDINGS

Chevron braced frames were designed for 3-, 6-, 9- and 12-story building configurations. For each configuration, separate designs were developed assuming R = 2 (R2), R = 3 (R3) and R = 4 (R4) with no seismic detailing, but accounting for some lateral capacity in the gravity system. The 12-story/R4 design was not included in this study since it resulted in smaller design forces than required by wind loads. A fourth design was developed for each configuration as a low-ductility dual system, with a primary braced frame system designed to resist wind only, and a relatively light moment frame reserve system (referred to here as a wind plus reserve system or WRS). OCBF designs according to the AISC seismic provisions were not included because the focus of this study was on chevron CBF R = 3 systems and their reliance on reserve capacity. Each of the 15 designs assumed the plan geometry of the SAC 9-story building (SAC, 2000b), with two braced frames per side. Consistent with the SAC 9-story building, each configuration assumed a first-story height of 18 ft, with 13-ft story heights above. See Figure 1 for a plan view and typical bracing elevations for the R2, R3 and R4 designs.

The frames were designed for Boston, Massachusetts in accordance with IBC 2006 and ASCE 7-05 using Load Resistance Factor Design (LRFD). The wind loads were determined using Exposure B. The seismic loads were determined using Site Class D and Seismic Design Category B, assuming no increase to the fundamental period as allowed by Section 12.8.2 of ASCE 7-05. Figure 2 plots

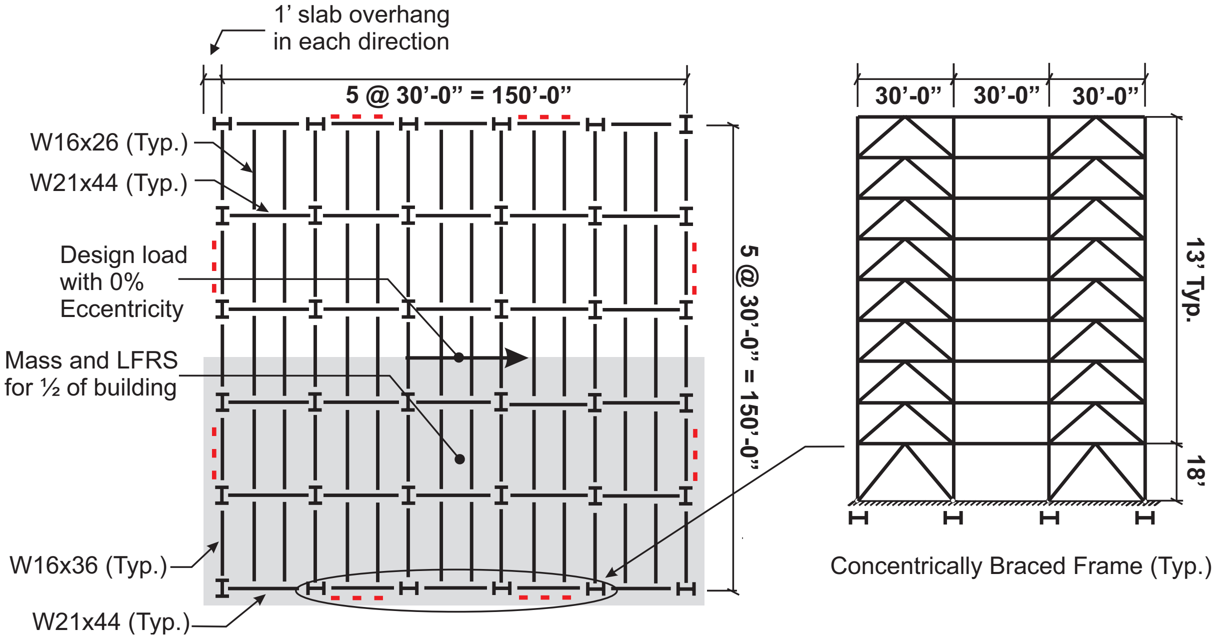

Fig. 1. R3 Plan view and 9-story braced frame elevation.

Table 2. R3 Design Member Sizes

Story (1)		Brace (2)	Girder (3)	Column (4)	Int. Grav. Col. (5)	Corner Col. (6)
3 Story 0.099(W)	R		W21x44			
	3	HSS 6x6x¼	W21x44	W12x40	W12x40	W12x40
	2	HSS 7x7x¼	W21x44	W12x40	W12x40	W12x40
	1	HSS 8x8x¼		W12x53	W12x53	W12x53
6 Story 0.066(W)	R		W21x44			
	6	HSS 6x6x¼	W21x44	W12x40	W12x40	W12x40
	5	HSS 6x6x¼	W21x44	W12x40	W12x40	W12x40
	4	HSS 7x7x¼	W21x44	W12x53	W12x53	W12x40
	3	HSS 8x8x¼	W21x44	W12x53	W12x53	W12x40
	2	HSS 8x8x¼	W21x44	W12x87	W12x87	W12x53
	1	HSS 8x8x5⁄16		W12x87	W12x87	W12x53
9 Story 0.050(W)	R		W21x44			
	9	HSS 6x6x¼	W21x44	W12x40	W12x50	W12x40
	8	HSS 6x6x¼	W21x44	W12x40	W12x50	W12x40
	7	HSS 7x7x¼	W21x44	W12x40	W12x50	W12x40
	6	HSS 7x7x¼	W21x44	W12x72	W12x72	W12x40
	5	HSS 8x8x¼	W21x44	W12x72	W12x72	W12x40
	4	HSS 8x8x¼	W21x44	W12x87	W12x87	W12x45
	3	HSS 8x8x¼	W21x44	W12x87	W12x87	W12x45
	2	HSS 8x8x¼	W21x44	W12x152	W12x136	W12x72
	1	HSS 9x9x5⁄16		W12x152	W12x136	W12x72
12 Story Design Base Shear = 0.040(W)	R		W21x44			
	12	HSS 5x5x¼	W21x44	W14x48	W14x48	W14x48
	11	HSS 6x6x¼	W21x44	W14x48	W14x48	W14x48
	10	HSS 7x7x¼	W21x44	W14x53	W14x61	W14x48
	9	HSS 7x7x¼	W21x44	W14x53	W14x61	W14x48
	8	HSS 7x7x¼	W21x44	W14x74	W14x82	W14x48
	7	HSS 8x8x¼	W21x44	W14x74	W14x82	W14x48
	6	HSS 8x8x¼	W21x44	W14x109	W14x109	W14x53
	5	HSS 8x8x¼	W21x44	W14x109	W14x109	W14x53
	4	HSS 8x8x¼	W21x44	W14x120	W14x109	W14x61
	3	HSS 8x8x5⁄16	W21x44	W14x120	W14x109	W14x61
	2	HSS 8x8x5⁄16	W21x44	W14x176	W14x145	W14x82
	1	HSS 9x9x5⁄16		W14x176	W14x145	W14x82

approximate base shear versus story height for wind and R3 earthquake loads according to these assumptions for buildings up to 18 stories. The close proximity of design earthquake and wind forces in this graph demonstrates the common experience in moderate seismic regions that wind can control member design, while seismic requirements control detailing. This is seldom the case in high seismic regions. Figure 2 also shows that the threshold at which wind forces control a design can vary depending on LRFD and Allowable Strength Design (ASD) approaches. For buildings that are not square, wind forces in the short direction control at lower heights.

Table 2 lists the member sizes for each R3 design. Brace sizes are listed in Column (2). All braces were designed as square HSS, slotted and field welded to gusset plates, as shown in Figure 3. All braces were selected to have a minimum thickness of ¼ in. Column (3) in Table 2 lists the braced frame girders. Column (4) lists the braced frame columns, designed to carry both gravity loads and overturning forces. Column (5) lists the interior gravity frame columns, and Column (6) lists corner columns, designed to carry gravity loads only. All beams and girders were designed assuming full composite action. The girders spanning between gravity frame columns were designed as W21×44s for vibration control. Spandrel girders were designed as W21×44s to meet deflection requirements. Although the gravity system was not designed explicitly for lateral loads, its lateral capacity was considered in the two dimensional (2D) analysis of the buildings by allowing these members to reach $0.20M_p$ with an elastic stiffness of $0.50EI$, based on a simplified interpretation of test results reported by Liu and Astaneh (2000). Gravity frame beams were designed as W16×26s and spandrel beams were designed as W16×36s, however, these beams were not modeled since the analyses assumed 2D seismic forces parallel to the girders.

Accounting for the expected yield strength and expected end fixity of the tube braces, the frame designs resulted in connections that fractured before the braces buckled. For this reason, brace buckling hysteresis and fracture life were not modeled. Instead the analytical model assumed elastic brace behavior up to fracture with little to no brace capacity thereafter (see Appendix). Table 3 compares the expected brace strength to the connection capacity for each R3 design. As a matter of convention, the R2, R4 and WRS designs were also assumed to experience connection fracture prior to brace buckling for all cases. Column (2) in Table 3 lists the computed LRFD axial brace force using ASCE 7-05 load combinations. Column (3) lists HSS members selected for an unbraced length between work points assuming an effective length factor for the brace of $K = 1.0$. The expected buckling strength of the braces [Column (4)] was calculated assuming an expected yield strength of $R_yF_y = (1.3)(46 \text{ ksi}) = 60 \text{ ksi}$, and using an effective length factor of $K = 0.7$. Column (5) lists the weld size used, representing one of four welds used for the connection shown in Figure 3.

Weld lengths were assumed to be at least the width of the HSS, consistent with requirements for plates in section J2.2b in the AISC *Specification* (AISC, 2005a) and similar recommendations extended to HSS in the AISC *Hollow Structural Section Connection Manual* (AISC, 1997b). Column (6) in Table 3 lists the assumed fracture capacity of the four welds listed in Column (5). For example the 3-story/R3 third story weld size listed in Column (5) is calculated as (0.6)(70 ksi)(3⁄16 in.)(0.707)(4)(6 in.) = 134 kips.

The wind plus reserve system (WRS) was designed with a primary chevron braced frame to resist wind only and two three-bay moment frames in each direction. See Figure 4 for the locations of the braced frames and moment frames, and see Table 4 for typical member sizes of the WRS designs. In order to change as few members as possible in the analytical model, the moment frames were constructed by moment connecting the existing spandrel girders in the braced frame. This "design" should be understood in diagrammatic and analytical terms only. In an actual building, complications might arise from attempting to moment connect large gusset plate connections without prequalified detailing. From an analytical point of view, imagining the new moment connections outside of the existing gravity framing system allowed the gravity beam contributions to remain identical between the two models. This study emphasized analytical comparisons of strength variations in primary and reserve LFRS, not the detailed implementation of an actual reserve system.

For the WRS design, the size of the braced frame columns was increased slightly to carry additional bending moments and to avoid extremely weak panel zones. The braced frame

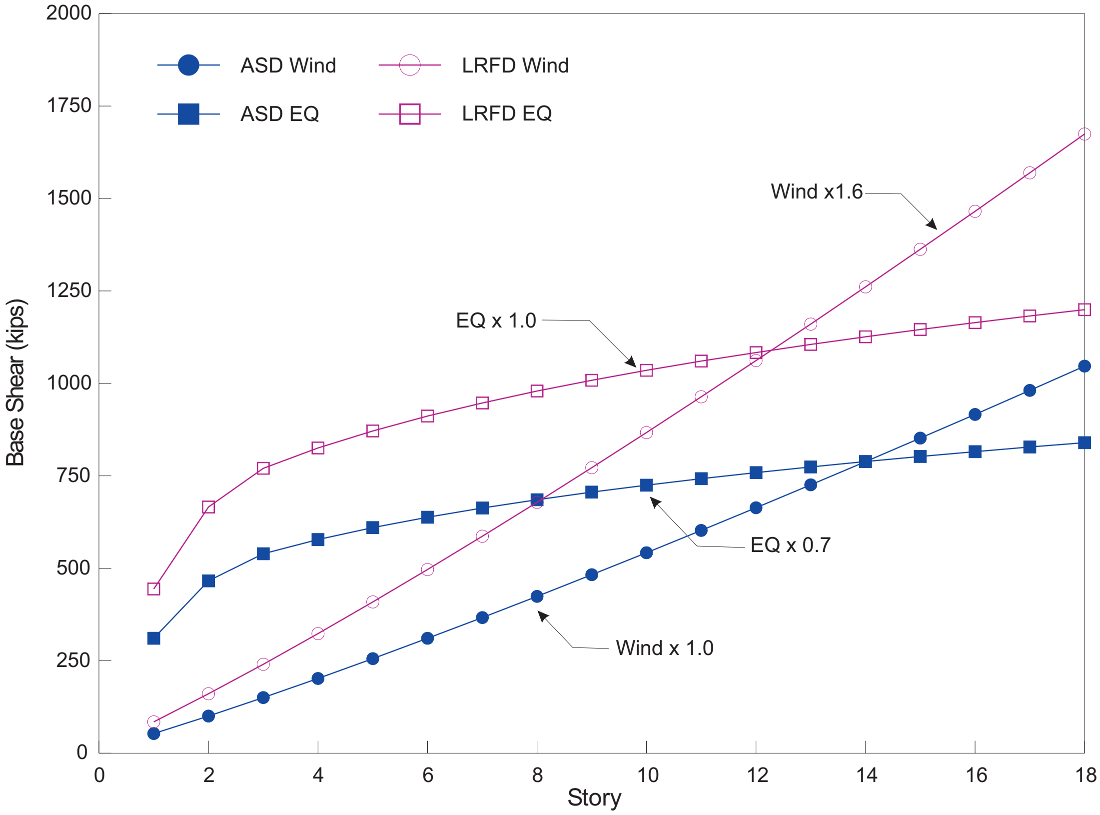

Fig. 2. R3 seismic and wind base shears with respect to story height.

Table 3. R3 Design Brace Sizes and Connection Forces

Story (1)		Design Load (2)	Brace (3)	Expected Strength (4)	Weld (×4) (5)	Weld Capacity (6)
3 Story	3	81 k	6x6x¼	201 k	3⁄16"x6"	134 k
	2	121 k	7x7x¼	268 k	¼"x7"	208 k
	1	158 k	8x8x¼	302 k	¼"x8"	238 k
6 Story	6	63 k	6x6x¼	201 k	3⁄16"x6"	134 k
	5	99 k	6x6x¼	201 k	3⁄16"x6"	134 k
	4	125 k	7x7x¼	268 k	¼"x7"	208 k
	3	153 k	8x8x¼	332 k	¼"x8"	238 k
	2	167 k	8x8x¼	332 k	¼"x8"	238 k
	1	197 k	8x8x5⁄16	371 k	¼"x9"	267 k
9 Story	9	62 k	6x6x¼	201 k	3⁄16"x6"	134 k
	8	95 k	6x6x¼	201 k	3⁄16"x6"	134 k
	7	119 k	7x7x¼	268 k	¼"x7"	208 k
	6	140 k	7x7x¼	268 k	¼"x7"	208 k
	5	158 k	8x8x¼	332 k	¼"x8"	238 k
	4	172 k	8x8x¼	332 k	¼"x8"	238 k
	3	182 k	8x8x¼	332 k	¼"x9"	267 k
	2	189 k	8x8x¼	332 k	¼"x9"	267 k
	1	218 k	9x9x5⁄16	453 k	¼"x10"	297 k
12 Story	12	57 k	5x5x¼	134 k	3⁄16"x5"	111 k
	11	87 k	6x6x¼	201 k	3⁄16"x6"	134 k
	10	110 k	7x7x¼	268 k	3⁄16"x7"	156 k
	9	130 k	7x7x¼	268 k	¼"x7"	208 k
	8	148 k	7x7x¼	268 k	¼"x7"	208 k
	7	163 k	8x8x¼	332 k	¼"x8"	238 k
	6	176 k	8x8x¼	332 k	¼"x8"	238 k
	5	186 k	8x8x¼	332 k	¼"x9"	267 k
	4	194 k	8x8x¼	332 k	¼"x9"	267 k
	3	200 k	8x8x5⁄16	409 k	¼"x9"	267 k
	2	204 k	8x8x5⁄16	409 k	5⁄16"x8"	297 k
	1	233 k	9x9x5⁄16	453 k	5⁄16"x9"	334 k

Table 4. WRS Design Member Sizes

Story (1)		Brace (2)	Girder (3)	Column (4)	Panel Zone Reduction (5)
3 Story	R		W21x44		$0.29M_p$
	3	HSS 5x5x¼	W21x44	W12x40	$0.29M_p$
	2	HSS 5x5x¼	W21x44	W12x40	$0.43M_p$
	1	HSS 6x6x¼		W12x72	
6 Story	R		W21x44		$0.29M_p$
	6	HSS 5x5x¼	W21x44	W12x40	$0.29M_p$
	5	HSS 5x5x¼	W21x44	W12x40	$0.37M_p$
	4	HSS 5x5x¼	W21x44	W12x50	$0.37M_p$
	3	HSS 6x6x¼	W21x44	W12x50	$0.57M_p$
	2	HSS 6x6x¼	W21x44	W12x96	$0.57M_p$
	1	HSS 7x7x¼		W12x96	
9 Story	R		W21x44		$0.34M_p$
	9	HSS 5x5x¼	W21x44	W12x53	$0.34M_p$
	8	HSS 5x5x¼	W21x44	W12x53	$0.34M_p$
	7	HSS 6x6x¼	W21x44	W12x53	$0.43M_p$
	6	HSS 6x6x¼	W21x44	W12x72	$0.43M_p$
	5	HSS 6x6x¼	W21x44	W12x72	$0.52M_p$
	4	HSS 7x7x¼	W21x44	W12x87	$0.52M_p$
	3	HSS 7x7x¼	W21x44	W12x87	$0.97M_p$
	2	HSS 7x7x¼	W21x50	W12x152	$0.84M_p$
	1	HSS 8x8x¼		W12x152	
12 Story	R		W21x44		$0.38M_p$
	12	HSS 5x5x¼	W21x44	W14x48	$0.38M_p$
	11	HSS 5x5x¼	W21x44	W14x48	$0.42M_p$
	10	HSS 6x6x¼	W21x44	W14x61	$0.42M_p$
	9	HSS 6x6x¼	W21x44	W14x61	$0.61M_p$
	8	HSS 6x6x¼	W21x44	W14x109	$0.61M_p$
	7	HSS 7x7x¼	W21x44	W14x109	$0.61M_p$
	6	HSS 7x7x¼	W21x44	W14x109	$0.61M_p$
	5	HSS 7x7x¼	W21x44	W14x109	$0.81M_p$
	4	HSS 8x8x¼	W21x44	W14x120	$0.81M_p$
	3	HSS 8x8x¼	W21x50	W14x120	$0.89M_p$
	2	HSS 8x8x¼	W21x62	W14x176	$0.67M_p$
	1	HSS 9x9x5⁄16		W14x176	

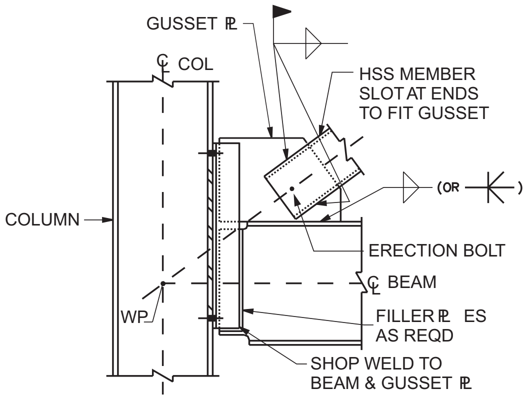

Fig. 3. Gusset plate connections. Note, the connection does not conform to the 2t brace-to-gusset plate requirement Fig. C-I-13.2 (AISC,2005b).

columns were initially designed to carry the gravity loads plus the overturning from wind only. They were then enhanced to withstand 0.01*g* acceleration, consistent with the minimum seismic force specified in Section 12.8.1.1 of ASCE 7-05. This load was distributed as an inverted triangle, assuming all braces had fractured and assuming no consideration for panel zone capacity. Since panel zone capacity ultimately controlled the strength of these reserve moment frames, beam yield strengths were reduced for analysis to the values listed in Column (5) of Table 4. In the taller configurations, the member size of the second-story braced/moment frame girder was increased for additional capacity. In addition to the reserve system, the WRS models were constructed to account for gravity framing reserve capacity in the same way as the R2, R3 and R4 designs. Furthermore, one line of gravity columns was rotated to act in the strong direction.

Table 5. Design Weight Comparison

		R2	R3	R4	WRS
3 Story	Lateral System Weight (tons)	53	44	42	44
	% Difference	22.3%	—	–3.7%	1.0%
6 Story	Lateral System Weight (tons)	107	98	93	94
	% Difference	9.3%	—	–5.1%	–4.3%
9 Story	Lateral System Weight (tons)	191	168	157	168
	% Difference	14.1%	—	–6.1%	0.3%
12 Story	Lateral System Weight (tons)	284	244	—	258
	% Difference	16.1%	—	—	5.4%

Table 5 compares the weights of the 15 lateral system designs, showing that in all cases the WRS designs are lighter than the R2 designs and very similar the to the R3 designs.

Reserve system first yield capacities of the models were assessed based on pushover analyses assuming control forces distributed as an inverted triangle and are reported in Table 6. Figure 5 shows the moment diagram for the 6-story/R3 pushover analysis. Note that the gravity framing provided enough stiffness to cause the braced frame columns to bend about their strong axis, effectively mobilizing column strength and stiffness at the first floor for columns assumed pin-connected to adjacent beams. Hence, even a modest reserve system can be expected to afford higher capacity than calculated simply according to beam yield strength.

Table 6. Reserve System First-Yield Capacities

		R3	WRS
No. of Stories	3	58 k	113 k
	6	80 k	132 k
	9	83 k	171 k
	12	85 k	176 k

Detailed discussion of the analytical models and ground motion suite can be found in the Appendix to this paper.

ANALYTICAL RESULTS

Collapse capacities of low-ductility structural systems are particularly sensitive to variations in both ground motion and building system characteristics. Furthermore, rock motions and soil amplification characteristics can vary greatly for a given MCE scenario. For these reasons, reliability-based performance assessments, such as described in FEMA-350 (SAC, 2000a) and ATC-63 (ATC, 2008), are particularly well-suited to evaluate the collapse capacities of low-ductility systems. The Appendix to this paper includes detailed discussion of both FEMA-350 and ATC-63 approaches to collapse performance assessment and explains why the ATC-63 approach was favored for these low-ductility systems. The Appendix also describes modifications to the ATC-63 approach that were necessary for accommodating special characteristics of the Eastern North America (ENA) suite and the low-ductility systems.

This section discusses structural behavior observed during analysis of these systems. Once the braces were assumed

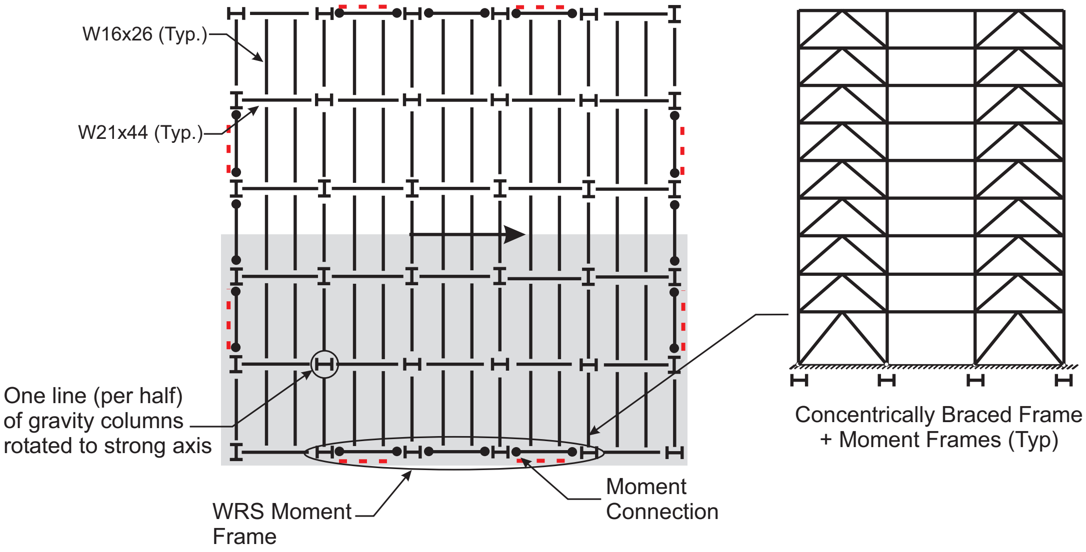

Fig. 4. WRS building plan and braced frame elevation.

to fracture, these systems experienced severe stiffness and strength discontinuities. System performance was highly dependent on ground motion characteristics. Different ground motions would fracture braces at different levels in different sequences, resulting in a variety of behaviors that are too complicated to characterize intuitively or simply. In spite of the complex behavior exhibited by these systems, however, some interesting behavioral trends did emerge out of both the analyses and the performance assessment process. Not only elastic higher mode effects, but also dynamically changing modes due to brace fracture were observed to affect collapse performance. Collapse performance was also observed to depend on building height, primary LFRS strength, and reserve LFRS strength.

Incremental dynamic analyses (IDAs) (Vamvatsikos and Cornell, 2002) were run for each of the 15 models under the 15 motions discussed in the Appendix, for a total 225 IDAs. Figure 6 shows the IDA results for the 9-story/R3 configuration. Starting at a scale factor (SF) of 1.0, the ground motion (GM) acceleration amplitudes for each IDA was scaled up

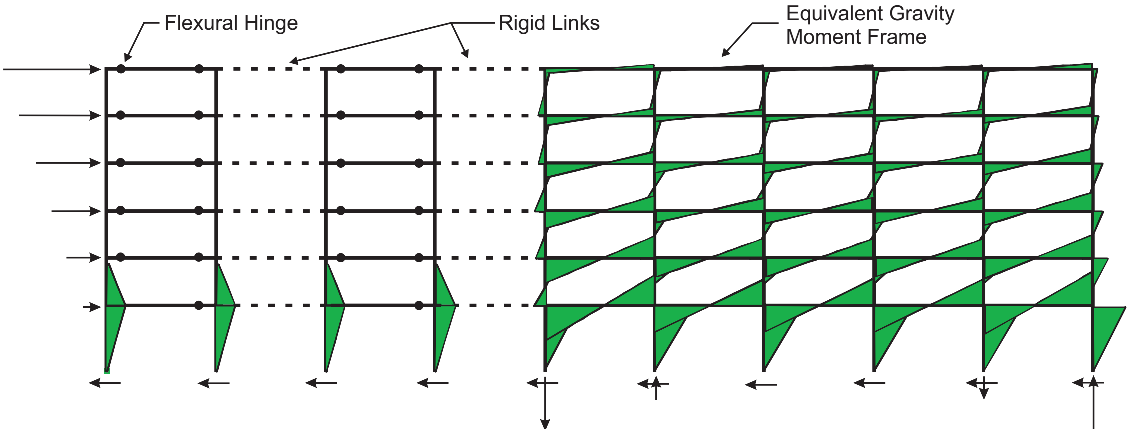

Fig. 5. Pushover analysis moment diagram for the 6-story/R3 reserve system.

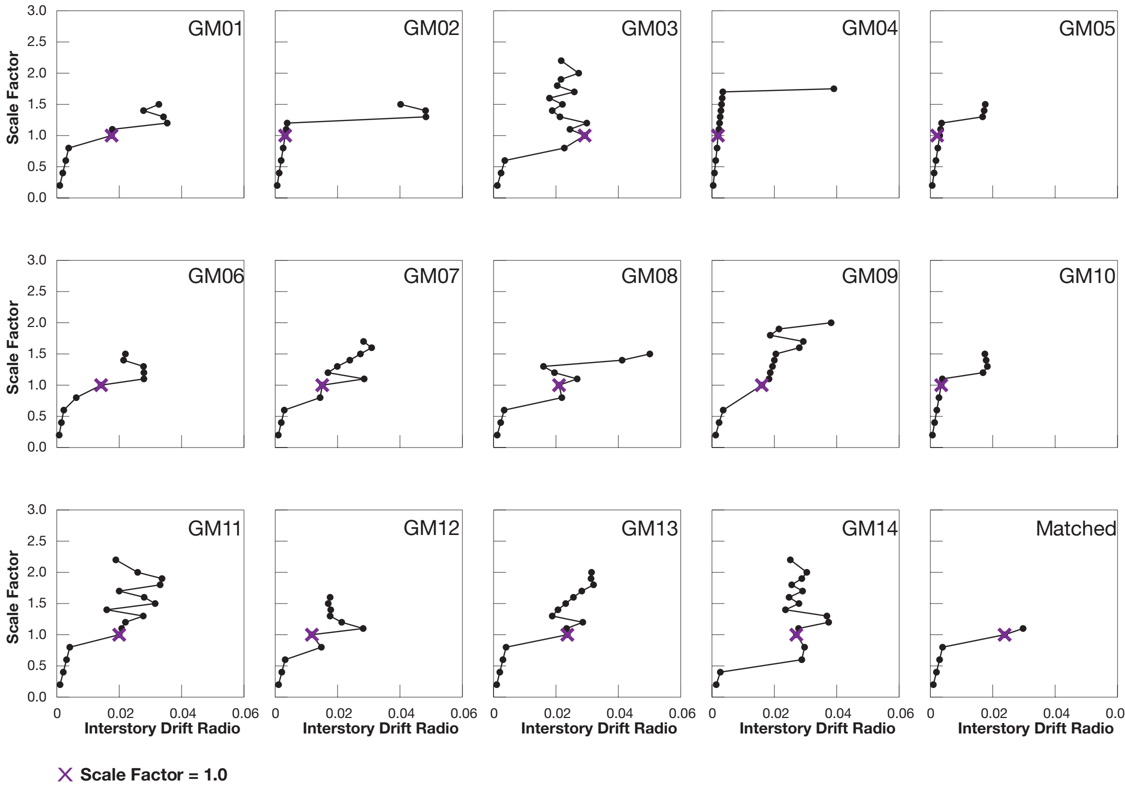

Fig. 6. IDA curves for the 9-story/R3 design.

Table 7. Collapse Table

	Design Value	Ground Motion														
		1	2	3	4	5	6	7	8	9	10	11	12	13	14	Matched
3 Story	WRS	6.8	6.8	5.8	4.5	5.0	4.5	4.5	2.8	5.4	8.0	4.5	5.8	6.0	4.5	3.0
	R4	1.2	1.9	0.8	1.7	1.5	1.6	2.8	2.0	2.4	0.8	1.6	1.8	2.4	1.0	1.2
	R3	0.8	1.1	0.8	1.3	0.8	1.4	3.0	1.0	1.2	1.2	1.3	0.6	1.4	0.8	0.8
	R2	0.6	2.4	1.3	1.4	1.6	1.2	1.8	1.1	0.8	1.7	1.7	1.7	1.5	0.8	1.3
6 Story	WRS	4.5	5.3	3.5	3.0	3.0	3.0	5.0	3.0	5.4	5.8	1.9	3.0	3.5	2.0	1.6
	R4	1.5	1.7	1.2	1.2	0.6	1.5	2.2	1.2	0.9	1.4	1.3	1.2	1.1	0.8	0.6
	R3	1.0	1.3	1.7	1.4	0.8	1.3	3.0	1.3	1.3	1.4	1.3	1.7	0.9	0.4	0.8
	R2	1.3	1.5	1.1	1.3	1.1	0.8	4.0	2.6	1.6	1.2	1.5	1.7	1.2	0.6	1.1
9 Story	WRS	4.5	6.0	5.0	3.5	3.5	3.0	4.5	1.8	5.8	5.2	6.0	4.0	4.5	2.6	1.2
	R4	1.2	1.9	1.3	1.5	1.3	0.8	1.4	1.5	1.5	1.2	3.0	1.4	1.3	1.2	0.8
	R3	1.5	1.5	1.5	1.7	1.5	2.2	1.8	1.5	2.0	1.5	2.2	1.6	2.0	2.2	1.1
	R2	2.6	2.6	2.8	2.6	1.4	1.5	3.0	2.2	4.0	1.7	1.4	3.5	2.0	1.4	1.3
12 Story	WRS	4.5	3.5	1.9	2.2	2.8	3.0	2.6	2.0	5.0	5.4	5.0	2.6	4.0	1.9	1.8
	R3	1.2	2.6	1.8	1.4	1.1	2.2	2.8	2.0	2.0	1.1	1.0	1.8	0.8	1.2	1.0
	R2	2.0	3.0	2.4	3.5	1.7	1.3	2.6	2.0	1.6	1.1	1.3	1.3	1.3	1.3	1.4

by increments of 0.1 until the model either collapsed or became numerically unstable, and it was scaled down until the model responded in the linear range. Some models required certain motions to be scaled down in order to arrive at their collapse capacity. Collapse capacity was recorded in terms of scale factor at the increment just prior to collapse. Note that incrementing SF rather than the spectral acceleration at the first natural period (S_{aT1}) was a modification to the ATC-63 process. The Appendix discusses this modification further.

Collapse capacities for each analysis are reported in Table 7, with a circle around analysis cases resulting in collapse at a scale factor of 1.0. Cases such as the 6-story/R3/GM1, with a collapse capacity of 1.0, survived the unscaled ground motion, but then collapsed when the ground motion was scaled to 1.1. Four models collapsed under the spectral matched motion, shown in Figure A-8 in the Appendix and listed in the column labeled “Matched” in Table 7. The highest IDA scale factor under this motion for the R2, R3 and R4 system designs was 1.4 for the 12-story/R2 design. IDA scale factors for the WRS designs under the matched motion ranged from 1.2 for the 9-story configuration to 3.0 for the 3- and 6-story configurations. Relatively poor performance under this motion suggests that the suite of motions used for this study should not be considered overly conservative. Furthermore, the choice of ground motions and soil amplification characteristics are essential to the collapse assessment of these systems. See the Appendix of this paper and Hines et al. (2009) for further discussion of ground motion suite selection for ENA.

The circled values in Table 7 give an immediate impression that the 3- and 6-story configurations were more vulnerable to collapse than the 9- and 12-story configurations. The 3-story/R3 model collapsed under 6 of the 15 unscaled ground motions (40%), whereas the 6-story/R3 model collapsed under 4 of the 15 unscaled ground motions (27%). The 9-story/R3 did not collapse under any unscaled ground motions and 12-story/R3 models collapsed under only one unscaled motion.

It is difficult to distinguish significant behavioral differences among the R2, R3 and R4 models for the 3- and 6-story configurations. For instance, the 3-story/R4 model collapsed under only two motions (13%), outperforming not only the 3-story/R3, but also the 3-story/R2 (three collapses = 20%). Such an observation suggests that collapse capacity may not always increase in proportion to strength. There may even be configurations, as demonstrated here, where an R3 design produces greater vulnerability than either a stronger or a weaker design.

Table 7 demonstrates the subtle relationship between design strength and collapse vulnerability via comparison of different designs under the same motion. For the 6-story configuration, GM5 collapsed only the weaker R3 and R4 designs. On the other hand, GM6 collapsed the stronger R2 design but spared the two weaker designs. In certain cases, the survival of a weaker design next to the collapse of a stronger design under the same ground motion can be understood by examining how initial damage protected the weaker design from subsequent stronger pulses by moving the building's natural periods out of the range of these pulses. For instance, the 6-story/R4 design experienced early damage at approximately 8 seconds into GM6, as shown in Figure 7. The first story drift record in Figure 7 shows that although the R4 model reached a drift of almost 3% as a result of this damage, the model righted itself under subsequent shaking. Conversely, the R2 design easily withstood the potentially damaging pulse at 8 seconds, only to collapse under much stronger shaking at 22 seconds.

The only 9-story configurations to collapse at SF = 1.0 were the R4 design under GM6 and the Matched motion, suggesting that for the taller configurations, increased strength played a role in mitigating collapse vulnerability. The 12-story/R3 design was observed to collapse under GM13 at the tenth story, demonstrating that taller buildings can become vulnerable to higher mode effects. This observation is consistent with observations from hundreds of analyses not reported in this paper on designs with lower brace capacities at higher stories (Appel, 2008). Brace connection capacities for the designs featured in this paper were specified according to fillet weld lengths equal to or in excess of the width of the brace. Table 3 demonstrates that the expected weld capacity in Column (6) typically far exceeded the demand on the brace in Column (2). For instance, for the 9-story/R3 model, Table 3 lists the seventh-story expected weld capacity as 208 kips, 1.75 times higher than the 119 kip design demand, whereas it lists the first-story expected weld capacity as 297 kips, only 1.36 times higher than the 218 kip design demand. Previous studies on designs with expected weld capacities uniformly proportional to design brace demands yielded more collapses in the upper stories and more uniform damage to the primary system. More uniformly distributed damage in the primary LFRS could serve to increase collapse capacity provided an appropriate reserve system is in place.

For all configurations, the WRS design significantly outperformed the strength designs experiencing no collapses at a scale factor of 1.0 and reaching median scale factors above 4.0. Figures 11 through 14 clearly demonstrate the robustness of the WRS designs in comparison to their strength design counterparts. The Appendix discusses these figures in greater detail. Figures 8 through 10 compare damage and collapse behavior of the 6-story/R3 and WRS designs. Figure 8 shows that the 6-story/R3/GM5 case experienced first brace fracture at the fifth story at around 7.6 seconds, with first-story brace fracture occurring at around 19.9 seconds in the negative direction. Subsequent pulses in the positive direction also fractured a second-story brace and yielded the second-story gravity frame prior to collapsing the model at the first story. Figure 9 shows that the 6-story/WRS/GM5 case also experienced first brace fracture at higher stories close to 7.5 seconds, with first-story brace fracture at around 15.4 seconds. No yielding of the reserve system and relatively low inelastic drifts, less than 0.5%, were observed. Figure 10 shows that the 6-story/WRS/GM5×2 case experienced more pronounced inelastic behavior when the GM5 accelerations were scaled to 2.0 times their original values.

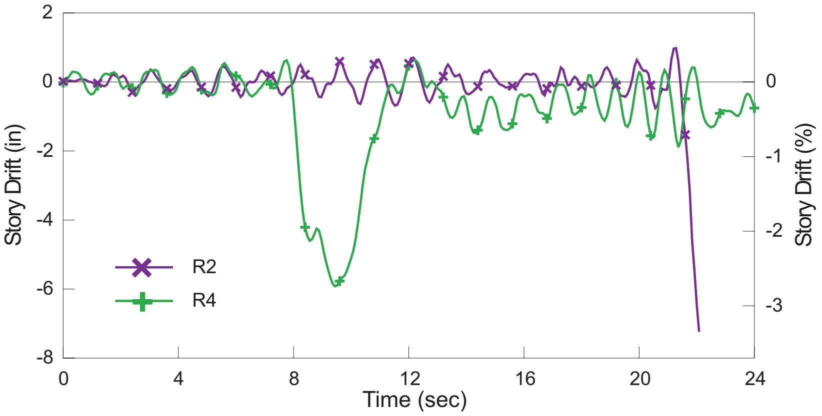

Fig.7. First-story drift for the 6-story/R2 and R4 models under GM6.

An additional brace fractured at the fifth story and reserve system beams were observed to yield at the second and fifth stories. Figure 10 demonstrates the need for some ductility in the reserve system. More ductile reserve systems allow IDAs to be scaled to higher levels. The same may also be said of stronger reserve systems, which are still significantly more flexible than the primary system. How reserve systems should be designed for strength and ductility presents itself as a major question for future research concerning low-ductility systems.

Collapse Performance Assessment

Figures 11 through 14 show not only the improvement to collapse capacity provided by the WRS designs for every configuration, but also the relative similarity between the R2, R3 and R4 designs. Note that the symbols in these figures are used to differentiate between curves. They do not represent experimental data points. For taller configurations, Figure 13 and Figure 14 demonstrate the beneficial effects of added strength, while they also show less difference between the R2 and WRS designs. Probability of collapse can be read for each design as the point where its fragility curve crosses the vertical line at an SF of 1.0. Figure 11 shows that the 3-story/R2, R3 and R4 designs appear to have collapse probabilities ranging from 30% to 48%, while the WRS design appears to have a collapse probability of less than 2%. While this study does not necessarily satisfy the further consideration required by ATC-63 for average and upper bound collapse probabilities for a set of "Index Archetype Configurations," the WRS results do generally fall under the recommended 10% threshold (ATC, 2008, p. 2-9). Figure 12 shows that the 6-story/R2, R3 and R4 designs appear to have collapse probabilities of about 40%, while the WRS curve shows a collapse probability of less than 10%. For the 9-story/R2, R3 and R4 designs, Figure 13 shows collapse probabilities ranging from 18% to 39%, while the WRS curve shows a collapse probability of 5%. Finally, Figure 14 shows collapse probabilities for the 12-story/R2 and R3 designs as 30% and 35%, while the WRS curve shows a collapse probability of 11%. While Table 7 lists only one collapse for the 12-story configuration at SF = 1.0, the WRS fragility curve in Figure 14 shows less dramatic improvement over the R2 and R3 designs. This can be explained by observing which stories collapsed at the maximum IDA increment for the various designs.

Tables 8 through 11 summarize the IDA results at the increment prior to collapse for each of the configurations. The "Scale Factor" rows in these tables present the same data as Table 7; however, these tables also list the story that collapsed and the maximum drift reached on this story at the increment before the collapse occurred. Note that the drift reported may not be the maximum drift, since it relates to

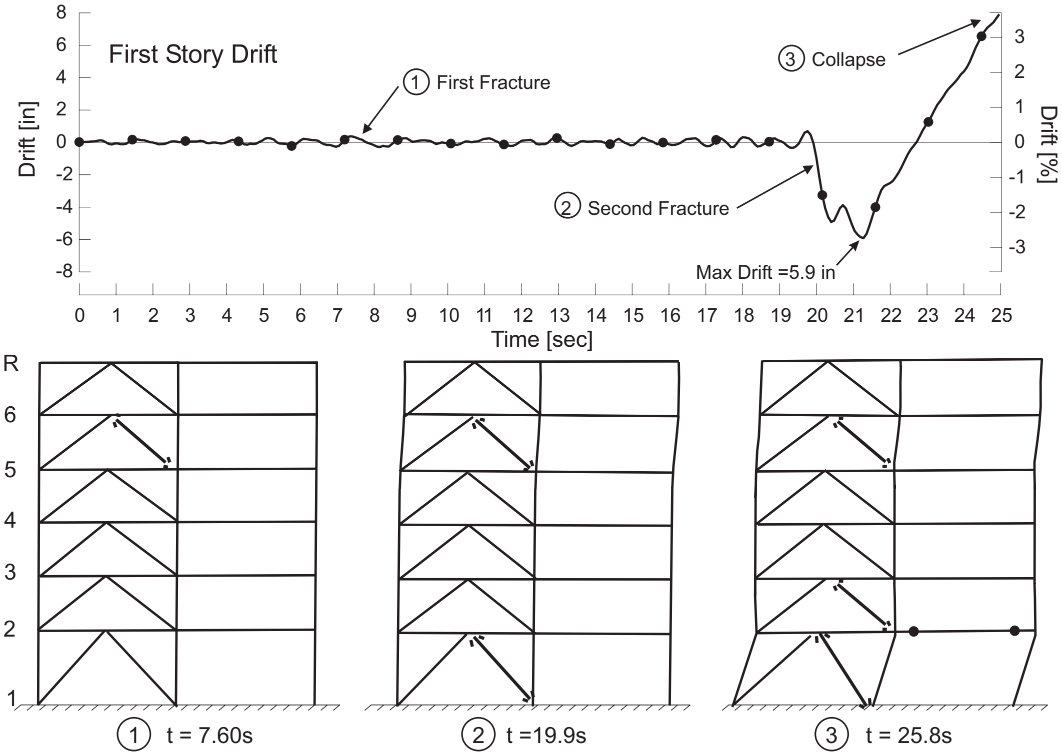

Fig. 8. Collapse behavior for 6-story/R3/GM5.

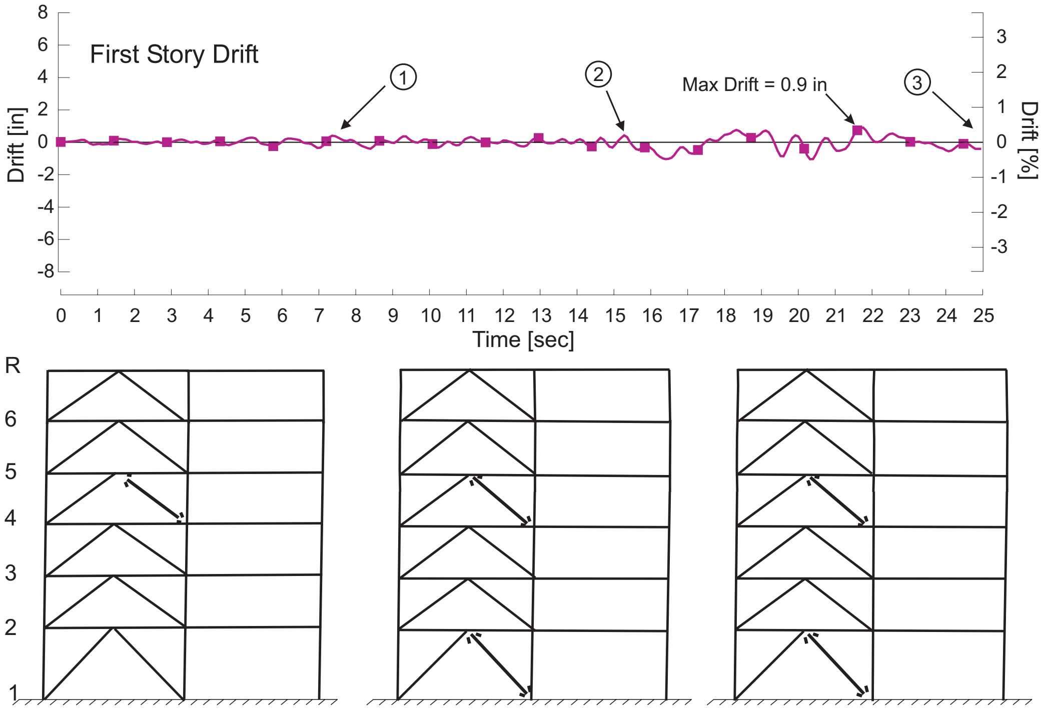

① t = 7.52s ② t = 15.4s ③ t = 25.4s

Fig. 9. Behavior for 6-story/WRS/GM5.

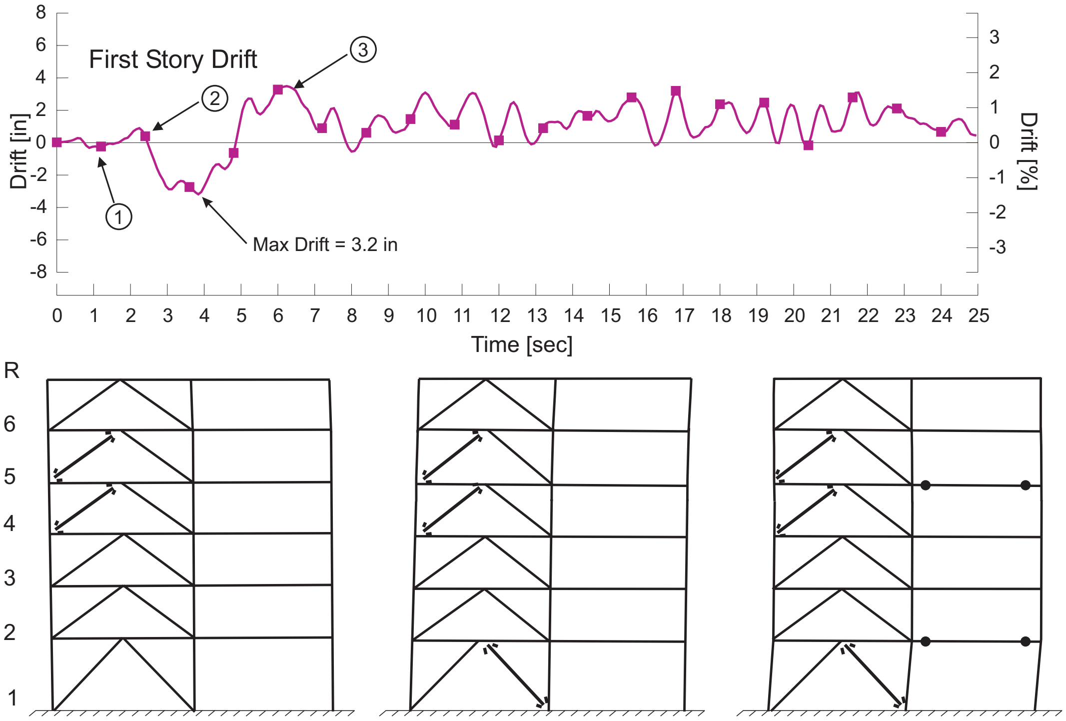

① t = 1.12s ② t = 2.00s ③ t = 6.32s

Fig. 10. Behavior for 6-story/WRS/GM5/SF = 2.0.

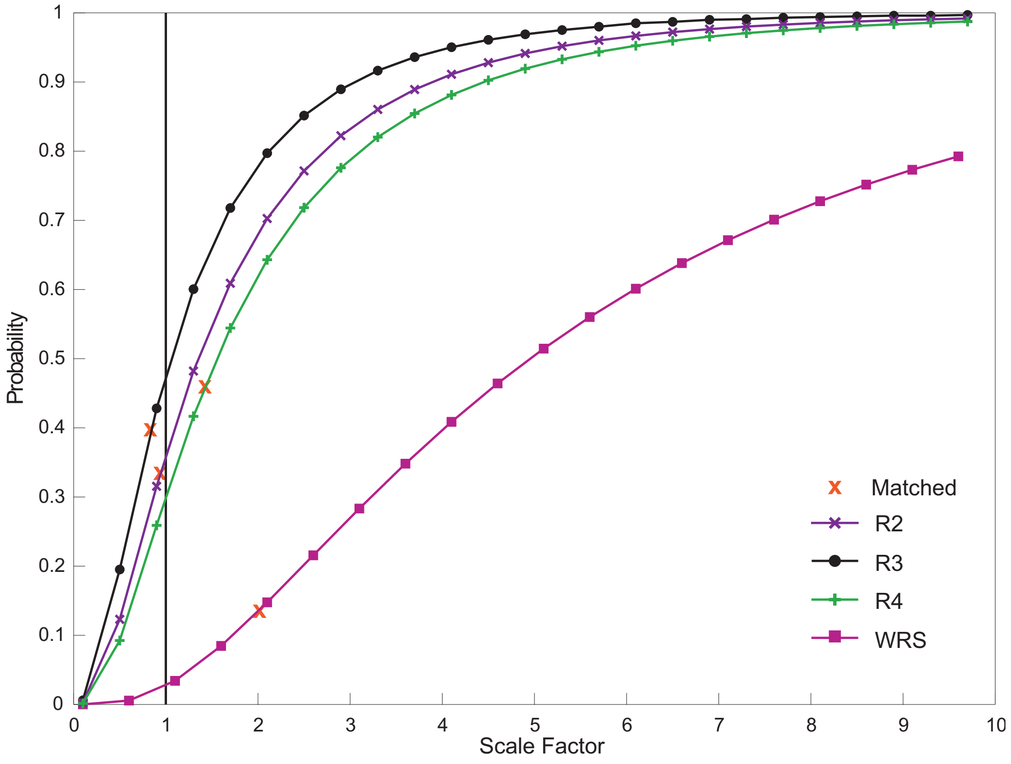

Fig. 11. 3-story fragility curves.

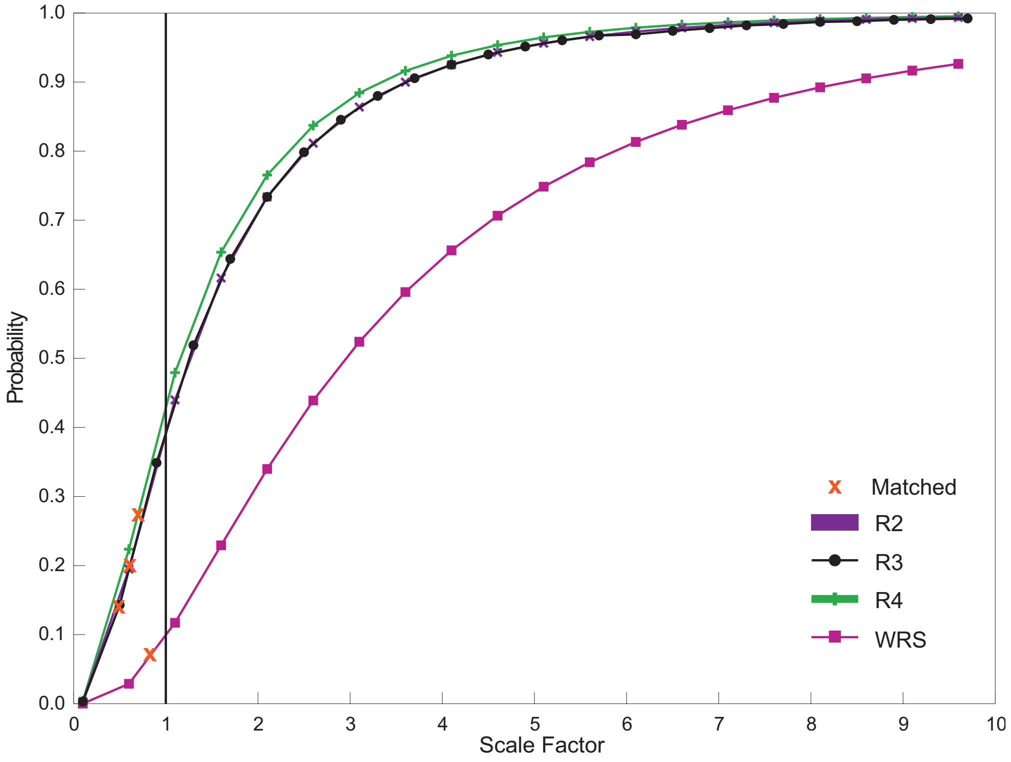

Fig. 12. 6-story fragility curves.

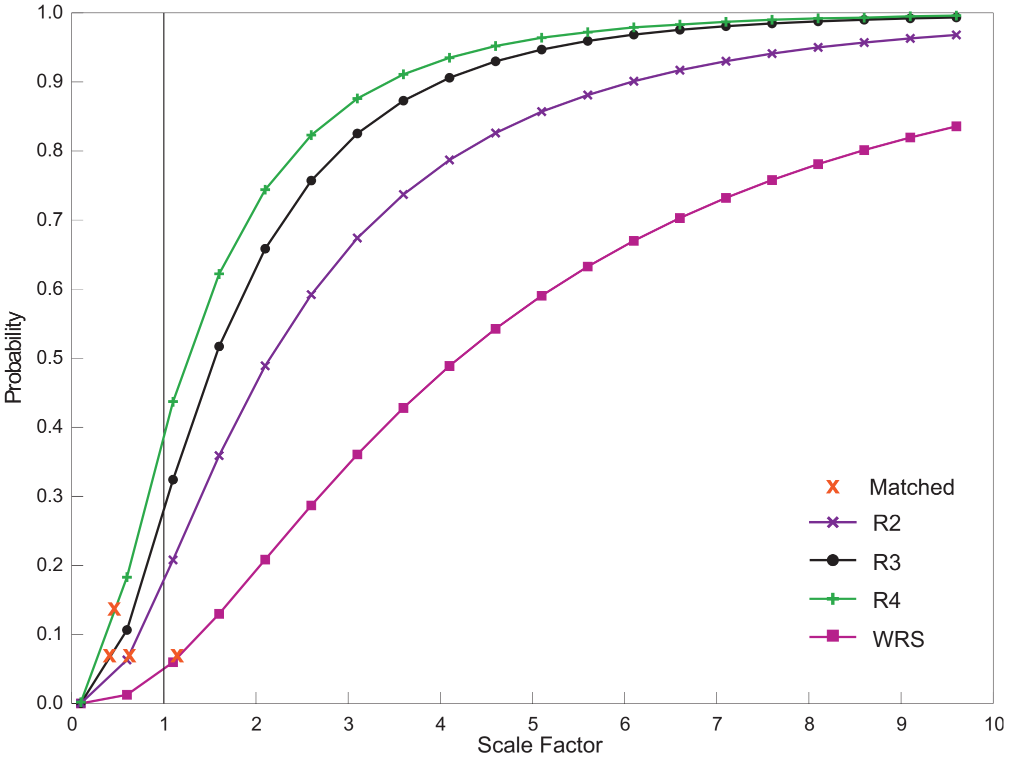

Fig. 13. 9-story fragility curves.

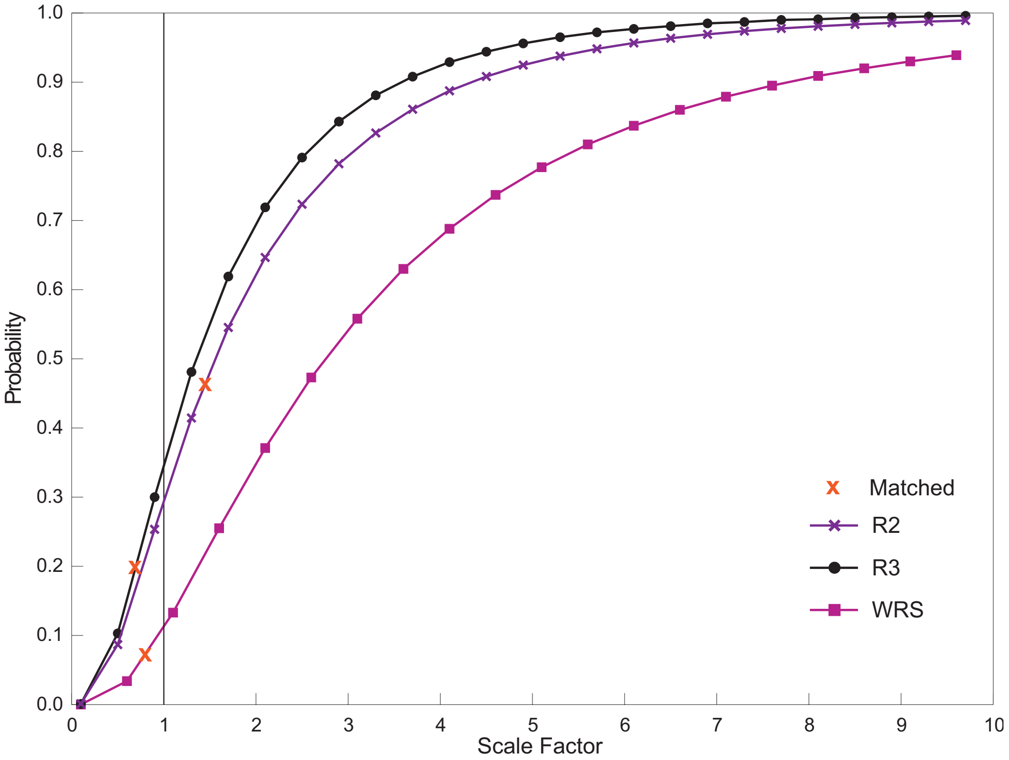

Fig. 14. 12-story fragility curves.

Table 8. 3-Story Collapse Summary

Design Value		Ground Motion														
		1	2	3	4	5	6	7	8	9	10	11	12	13	14	Matched
R2	Story	1	1	1	3	1	3	1	1	3	3	1	1	1	1	1
	Scale Factor	0.6	2.4	1.3	1.4	1.6	1.2	1.8	1.1	0.8	1.7	1.7	1.7	1.5	0.8	1.3
	Drift	.011	.055	.031	.027	.039	.027	.023	.021	.016	.029	.024	.037	.019	.038	.032
R3	Story	1	1	1	1	1	1	1	1	1	1	1	1	1	1	1
	Scale Factor	0.8	1.1	0.8	1.3	0.8	1.4	3.0	1.0	1.2	1.2	1.3	0.6	1.4	0.8	0.8
	Drift	.032	.018	.015	.027	.016	.035	.038	.028	.030	.012	.044	.026	.017	.037	.002
R4	Story	1	1	1	1	1	1	1	1	1	1	1	1	1	1	1
	Scale Factor	1.2	1.9	0.8	1.7	1.5	1.6	2.8	2.0	2.4	0.8	1.6	1.8	2.4	1.0	1.2
	Drift	.031	.019	.025	.022	.022	.027	.029	.028	.014	.021	.020	.022	.026	.036	.023
WRS	Story	1	1	1	1	1	1	1	1	1	1	1	1	1	1	1
	Scale Factor	6.8	6.8	5.8	4.5	5.0	4.5	4.5	2.8	5.4	8.0	4.5	5.8	6.0	4.5	3.0
	Drift	.037	.044	.038	.022	.042	.026	.030	.030	.018	.026	.021	.035	.043	.026	.044

Table 9. 6-Story Collapse Summary

Design Value		Ground Motion														
		1	2	3	4	5	6	7	8	9	10	11	12	13	14	Matched
R2	Story	5	1	6	1	1	4	1	1	1	4	1	1	1	1	1
	Scale Factor	1.3	1.5	1.1	1.3	1.1	0.8	4.0	2.6	1.6	1.2	1.5	1.7	1.2	0.6	1.1
	Drift	.037	.009	.013	.034	.011	.005	.031	.038	.035	.029	.030	.055	.036	.022	.005
R3	Story	5	1	1	1	1	1	1	1	1	5	1	1	1	1	1
	Scale Factor	1.0	1.3	1.7	1.4	0.8	1.3	3.0	1.3	1.3	1.4	1.3	1.7	0.9	0.4	0.8
	Drift	.023	.023	.027	.035	.023	.040	.014	.017	.028	.018	.033	.029	.012	.014	.018
R4	Story	1	1	1	1	1	5	1	1	1	1	1	1	1	1	1
	Scale Factor	1.5	1.7	1.2	1.2	0.6	1.5	2.2	1.2	0.9	1.4	1.3	1.2	1.1	0.8	0.6
	Drift	.016	.017	.017	.016	.003	.019	.026	.025	.011	.028	.018	.035	.047	.030	.003
WRS	Story	1	1	1	1	1	1	1	1	1	1	1	1	1	1	1
	Scale Factor	4.5	5.0	3.5	3.0	3.0	3.0	5.0	3.0	5.4	5.8	1.9	3.0	3.5	2.0	1.6
	Drift	.015	.023	.022	.026	.021	.024	.048	.027	.033	.022	.017	.029	.024	.021	.047

Table 10. 9-Story Collapse Summary

Design Value		Ground Motion														
		1	2	3	4	5	6	7	8	9	10	11	12	13	14	Matched
R2	Story	8	1	1	1	8	7	1	1	1	1	9	1	8	7	1
	Scale Factor	2.6	2.6	2.8	2.6	1.4	1.5	3.0	2.2	4.0	1.7	1.4	3.5	2.0	1.4	1.3
	Drift	.057	.035	.018	.027	.031	.031	.028	.027	.030	.026	.027	.023	.026	.046	.005
R3	Story	8	1	1	1	8	1	1	1	9	1	8	8	1	1	1
	Scale Factor	1.5	1.5	1.5	1.7	1.5	2.2	1.8	1.5	2.0	1.5	2.2	1.6	2.0	2.2	1.1
	Drift	.033	.040	.022	.028	.050	.022	.039	.018	.038	.018	.019	.018	.031	.025	.030
R4	Story	7	1	1	1	7	1	1	1	1	7	1	1	1	1	1
	Scale Factor	1.2	1.9	1.3	1.5	1.3	0.8	1.4	1.5	1.5	1.2	3.0	1.4	1.3	1.2	0.8
	Drift	.027	.018	.017	.026	.018	.017	.004	.031	.022	.042	.020	.018	.018	.019	.021
WRS	Story	1	1	1	1	1	1	1	1	1	1	1	1	1	1	1
	Scale Factor	4.5	6.0	5.0	3.5	3.5	3.0	4.5	1.8	5.8	5.2	6.0	4.0	4.5	2.6	1.2
	Drift	.027	.031	.035	.036	.024	.022	.039	.030	.021	.024	.017	.034	.024	.019	.020

Table 11. 12-Story Collapse Summary

Design Value		Ground Motion														
		1	2	3	4	5	6	7	8	9	10	11	12	13	14	Matched
R2	Story	1	9	1	1	1	12	11	11	11	11	1	11	11	1	1
	Scale Factor	2.0	3.0	2.4	3.5	1.7	1.3	2.6	2.0	1.6	1.1	1.3	1.3	1.3	1.3	1.4
	Drift	.041	.029	.019	.032	.028	.028	.028	.020	.023	.028	.043	.016	.051	.043	.029
R3	Story	11	1	11	12	1	1	1	11	1	1	1	1	10	1	11
	Scale Factor	1.2	2.6	1.8	1.4	1.1	2.2	2.8	2.0	2.0	1.1	1.0	1.8	0.8	1.2	1.0
	Drift	.022	.023	.011	.017	.027	.026	.020	.036	.021	.023	.026	.015	.017	.017	.014
WRS	Story	1	1	1	1	1	1	1	1	1	1	1	1	1	1	1
	Scale Factor	4.5	3.5	1.9	2.2	2.8	3.0	2.6	2.0	5.0	5.4	5.0	2.6	4.0	1.9	1.8
	Drift	.015	.024	.022	.017	.024	.018	.014	.032	.015	.022	.018	.018	.022	.024	.014

the story that collapsed in the next increment, and not the story with maximum drift in the increment reported. Table 11 lists all maximum IDA increment collapses on the first story for the 12-story/WRS model, whereas it lists 8 out of 15 collapses at higher stories for the R2 design and 6 out of 15 collapses at higher stories for the R3 design. The WRS design still outperformed both R2 and R3 designs, and effectively prevented collapses at upper stories due to higher mode effects. The strength and stiffness of the WRS reserve system were, however, insufficient to allow IDA amplification levels similar to shorter buildings. This can be explained by the large P–Δ effects at the first story under the heavy weight of the 12-story structure. Even though shear forces between the first and second stories were lower in proportion to total weight for the 12-story configurations, lack of fixity at the column bases and increased story height made the reserve system more vulnerable to P–Δ effects and less able to handle amplified forces and deformations after brace fracture. In fact, Tables 8 through 11 list all IDA maximum increment collapses for the WRS on the first story, demonstrating that this problem of a soft story in the reserve system ultimately proved to limit all of the WRS designs. For taller configurations, the problem became more pronounced due to higher gravity loads. Such a result makes intuitive sense, and is certainly familiar from experience with more ductile systems in high seismic regions. This result leads to three questions about reserve systems that should direct further investigation:

1. For taller structures, how effective are primary system strength and reserve system strength and stiffness at the lower stories in preventing collapse?

2. Performance of reserve systems for individual structures can be improved by tuning based on nonlinear dynamic analysis, but can simpler, more realistic tuning methods be developed?

3. Would it be advantageous not to specify minimum weld requirements for upper story braces?

The third question arises out of previous work where model brace fracture capacities were based on brace design forces, rather than on minimum weld lengths. These analyses allowed more uniform damage throughout the structure and concentrated more maximum increment IDA collapses in the upper stories, where P–Δ effects were smaller than the lower stories and where increases in reserve system strength and stiffness are potentially less costly. These three questions help to emphasize that while this study has indicated the possibility of improved performance with reserve systems, it has neither demonstrated ideal reserve system designs nor determined the minimum acceptable capacity for reserve systems. The reserve system is a broad and flexible concept that appears essential to the design of low-ductility structures in moderate seismic regions, but it requires further investigation to be developed for general use in design.

CONCLUSIONS

Moderate seismic regions are distinguished from high seismic regions in three basic ways.

1. Collapse prevention, rather than potential economic loss, drives lateral system design.

2. Ground motions for moderate seismic regions differ significantly from their high seismic counterparts.

3. Wind loads and stiffness considerations often govern system choice and member design.

In light of these differences it is reasonable to talk about an independent seismic design philosophy for low-ductility structures in moderate seismic regions. At the heart of this philosophy, the concepts of reserve capacity and elastic flexibility should complement more well-established concepts of strength, ductility and capacity design. Such a philosophy should provide engineers with maximum flexibility for developing new structural systems based on first principles. This paper focused specifically on the concept of reserve capacity and its ability to enhance collapse performance for chevron braced steel frames not specifically detailed for seismic resistance.

R = 3 designs for 3-, 6-, 9- and 12-story building configurations under 2% in 50-year earthquake loads calculated according to IBC 2006 were assessed to have an approximately 30% chance of collapse for a typical Site Class D location in Boston, Massachusetts. Two major assumptions in this study violated ATC-63 recommendations for collapse performance assessment (ATC, 2008):

1. The gravity system provided reserve capacity (p. 1-4).

2. Suite ARS values were allowed to be uniformly lower than their IBC 2006 counterparts at the building fundamental period (p. A-11).

The R = 3 models would have demonstrated less robust collapse performance without these two assumptions.

At the same time, conventional faith in the collapse resistance of low-ductility steel structures appears to be well founded. For instance, Yanev et al. (1991) noted that the performance of steel structures has been excellent in previous earthquakes, with very few actual collapses. Steel building collapses were generally concentrated in the 1985 Mexico City earthquake, where most steel frames had been constructed out of built-up sections rather than rolled shapes. No steel structures were observed to collapse during the Northridge earthquake (Bruneau et al., 1995), and the only steel braced frames structures that collapsed during the

Kobe earthquake had been braced with rods, angles and flat bars (Tremblay et al., 1996). Nevertheless, the literature is relatively silent both on why these low-ductility buildings designed for high seismic regions survived and on whether such anecdotes constitute reliable assurance that a provision such as $R = 3$ will prevent future collapses. Large-scale test data related to the performance of sections and details typically used for building design in moderate seismic regions, as well as large-scale shaking table tests related to the collapse of low-ductility frames are only sparsely addressed in the literature to date.

In this study, the $R = 3$ models' resistance to collapse appears to have derived more from their inherent elastic reserve capacity than from their inherent ductility. Changes in primary LFRS strength, explored for $R = 2$ and $R = 4$ designs neither significantly improved nor significantly degraded collapse performance. In fact, the 3-story/R4 model outperformed both of the stronger designs. Changes to the reserve system capacity, however, uniformly improved collapse performance. The familiar concept of reserve capacity is widely accepted for high-ductility dual systems, and it is implied in the $R = 3$ provision itself. As a philosophical concept, reserve systems have the potential to increase safety, reduce construction cost, and encourage innovation in LFRS design. With so much riding on reserve systems, they should be recognized formally and designed explicitly.

Further investigation of these questions requires more complete understanding of low-ductility structural details and their effects on system collapse performance. Bruneau et al. (1995) noted that 4 out of 11 CBFs observed after the Northridge earthquake experienced some form of anchor bolt yielding or failure. Gravity column splices could also hasten collapse if they act as weak links during the engagement of the gravity frame as a reserve system. Conversely, gusset plate connections could be designed to provide significant strength and ductility via moment frame action after brace fracture.

We recognize the multiple uncertainties associated with the study presented in this paper and feel that questions related to the collapse performance of $R = 3$ chevron braced steel frames will remain difficult to answer definitively. In spite of these uncertainties, however, it is our opinion that these analyses demonstrate the potential for reserve systems to improve $R = 3$ collapse performance significantly. In fact, an appropriate reserve system could allow the primary LFRS to be designed for wind only, effectively reducing overturning demands on a building's foundation.

The models presented in this paper were created from the same template, varying only in configuration, member sizes and the extent of reserve system. Assumptions regarding nonlinear material and geometric behavior were uniform for all models. Therefore, the improvement in analytical collapse performance achieved through more robust reserve systems was interpreted as insight into actual physical behavior. While it is possible to debate the reserve capacity assumed in these models for gravity framing or gusset plate connections, it is likely that the concept of a reserve system itself is quite reasonable. Ideally, future research will encourage the development of typical details for gusset plate connections that allow them to be included fully in the reserve system. If it can be clearly understood how much reserve capacity is required to ensure adequate collapse performance, then a structural designer may be able to create a reserve system via typical gusset plate details without adding more moment connections. Additional reserve system capacity may only be necessary in the weakest areas of a structure, allowing such a system to be tuned for efficiency. Philosophical emphasis should be placed on the need for a reliable reserve system. The manner in which a particular system is to be achieved should remain the responsibility of the designer.

In response to the lack of literature discussing the $R = 3$ criterion and low-ductility collapse performance under moderate seismic excitation in general, this study has called attention to questions that fall outside the general conceptual framework for design in high seismic regions:

1. What are the relationships among strength, ductility, elastic flexibility, reserve capacity, damage and collapse for low-ductility systems?

2. How can understanding of these relationships be used to develop an appropriate design philosophy for low-ductility systems in moderate seismic regions?

Such a philosophy should ensure safety, promote economy and allow designers maximum flexibility to develop creative structures that resist collapse. We hope that our discussion of the reserve system concept will serve as a useful step toward defining this philosophy.

ACKNOWLEDGMENTS

Funding for this work was provided jointly by the American Institute of Steel Construction, LeMessurier Consultants, the Structural Steel Fabricators of New England, the Boston Society of Architects, and the Boston Society of Civil Engineers. The authors would like to thank M.C. Gryniuk for his work in developing the original Ruaumoko braced frame models that were modified for this study and for helping to select an appropriate hysteresis rule for fracturing braces; R.A. Henige, LeMessurier Consultants, for his input on the building design and analysis; S. Sorabella and L.G. Baise, Tufts University, for their work on developing the ground motion suite; R. Leon for his helpful comments regarding analysis of OCBF systems; and the AISC Research Advisory Committee for their many helpful comments on earlier drafts.

Table A-1. Modeling Assumptions

	Assumption	Conservative or Unconservative	Comments
1	2D behavior	Unconservative	Torsional behavior can amplify force and deformation demands.
2	No nonstructural components	Unconservative/ Conservative	Unconservative if such elements serve to concentrate stiffness and attract loads to vulnerable parts of the building, or reduce the period of the structure. Conservative if such elements provide reserve capacity.
3	No flexural stiffness or strength of gusset plate connections	Conservative	Gusset plate-to-column connections are not expected to behave reliably in a ductile manner. While it may be possible for them to provide reserve capacity before fracturing, this reserve capacity is not well understood.
4	No buckling of columns	Unconservative	Stronger braces and connections could overload columns.
5	Perfect anchorage of column bases	Unconservative/ Conservative	Unconservative if yielding of anchor rods results in displacement of the building column on top of a concrete pier; conservative if yielding of anchor rods allows the primary LRFS to rock before experiencing significant damage.
6	Strong column splices	Unconservative	The column splices are allowed to develop the full flexural strength of the smallest member.
7	Gravity frame girders have 0.50EI, yield at 0.2M_p, and have high ductility	Conservative	According to Liu and Astaneh (2000), 30% to 40% capacity is only available for certain size members and for the load direction where the slab goes into compression. The capacity drops to approximately 18% at relatively low levels of inelastic rotation. See further discussion later.
8	The SAC building geometry is highly regular	Unconservative	This level of regularity in a building system cannot be considered typical, especially in a moderate-to-low-seismic region.
9	Braced frame columns bent about strong axis and gravity columns bent about weak axis; gravity girders (not beams) to be oriented parallel to direction of loading	Conservative/ unconservative	All columns were allowed to yield in flexure as beam-columns. For an R3 system, a designer theoretically assumes no responsibility for the orientation and contribution of the gravity framing as a reserve system.
10	The models do not lose all brace capacity immediately after reaching their designated fracture force	Unconservative	This assumption was necessary to ensure reliable numerical convergence. See further discussion that follows.

APPENDIX

Design and Modeling of Braced Frame Buildings

Half of each building configuration (Figure 1 and Figure 4) was modeled using the nonlinear analysis software Ruaumoko-2D (Carr 2004). The braced frames were connected by rigid links to a moment frame representing the inherent lateral capacity of the gravity framing (Figure 5). Table A-1 lists major assumptions applied consistently throughout the study. These assumptions are neither uniformly conservative nor uniformly unconservative.

Assuming that the girders yield at 0.20M_p (assumption 7) could be unconservative, because the gravity loads on the girders did not require their connection to be developed over the full depth of the W21×44. Liu and Astaneh's (2000) tests, however, generally assumed full depth connections. The gravity framing and reserve systems were modeled with bilinear plastic hinging mechanisms in the beams and columns (Figure A-1). Each girder modeled in the gravity frame represented two girders in order to capture the two lines of gravity framing. Girder yield moment capacity was therefore (50 ksi)(0.2)(95.4 in^3)(2) = 1910 kip-in.

Due to large discontinuities in strength and stiffness between damaged and undamaged frames, it was difficult to get these systems to converge numerically. The braces were modeled using the Ruaumoko model for the Matsushima strength reduction hysteresis rule (Matsushima, 1969). The braces were assumed not to lose all brace capacity immediately after reaching their designated fracture force, rather they assumed a constant yield plateau prior to the first reversal of force. After the first reversal this yield plateau was abandoned and the brace was assumed to degrade to 5% of its previous strength. Each further reversal prompted an additional 95% degradation, effectively modeling zero capacity after the first excursion. While such yielding is unrealistic for braces prone to fracture, it did not appear to have a major impact on system performance. Figure A-2 represents a typical case where such yielding appears significant in the context of a hysteresis loop, but seems less so when observed as a function of time (Figure A-3, Figure A-4).

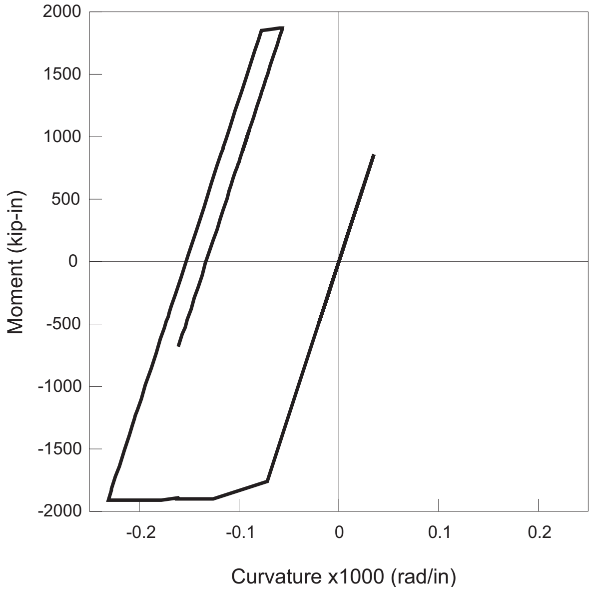

Fig. A-1. A 6-story/R3/GM3 second-floor bilinear hysteresis loop representing two gravity girders.

Figure A-3 plots force as a function of time for similar braces in three different structures: R3 with the brace hysteresis rule described earlier, designated *R3*; R3 with a bilinear brace hysteresis rule, designated *bilinear*; and the WRS system. As Figure A-3 shows, the two R3 structures demonstrated similar elastic behavior up to first-fracture/first-yield at approximately 4.7 seconds. The displacement response histories for these same situations are shown in Figure A-4. The R3 brace continued to resist force for approximately 1 second thereafter, before reaching a steady state of effectively zero force. The bilinear brace continued to resist force, without experiencing significant yielding. The WRS brace closely followed both R3 braces in the elastic range up to first fracture, continuing to resist force for approximately 1 second thereafter before reaching a steady state of zero force. While this short period of residual brace capacity may not represent physical behavior, it accounts for only a fraction of the total response over time and is less alarming

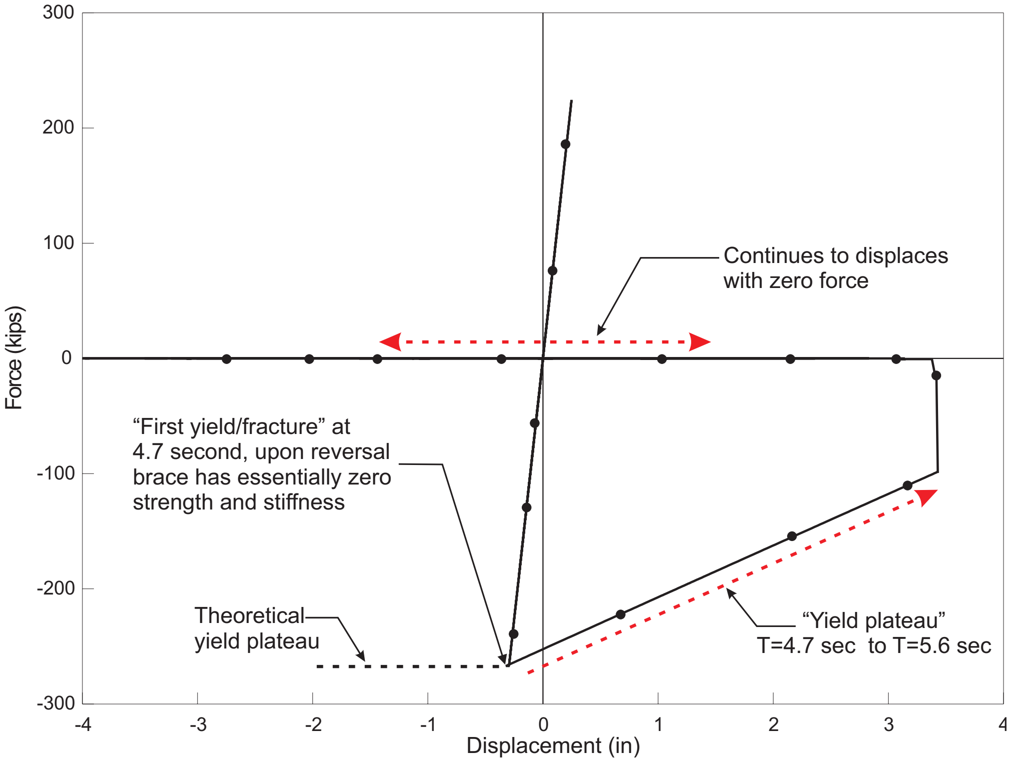

Fig. A-2. A 6-story/R3/GM3 first-story brace hysteresis loop.

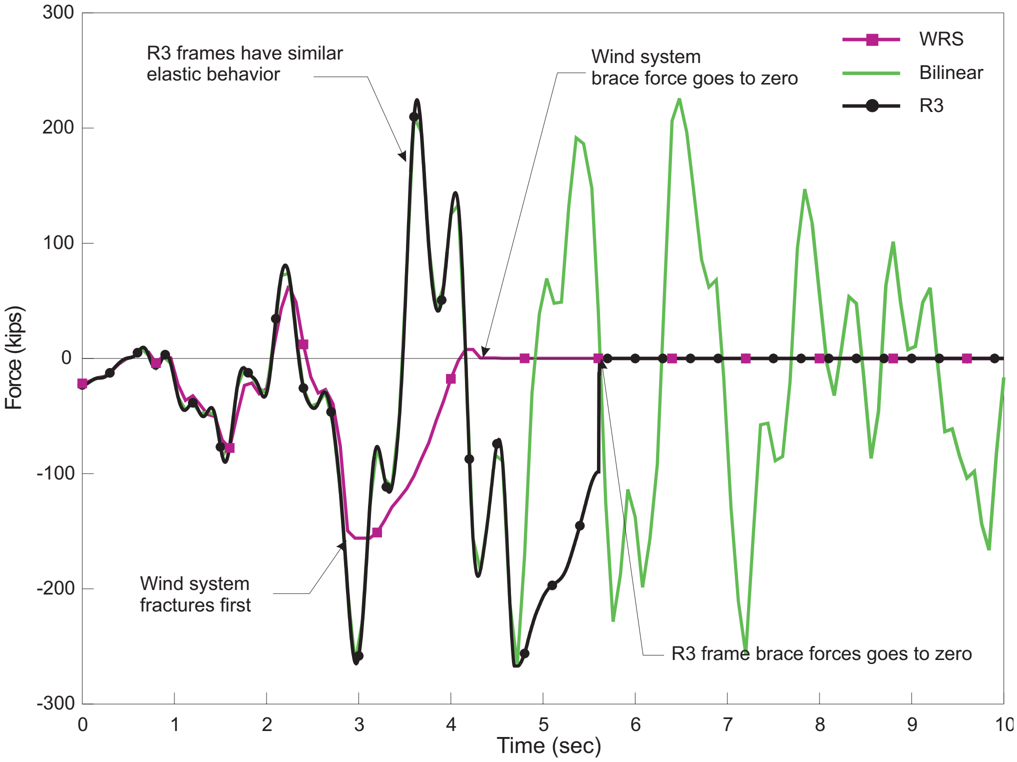

Fig. A-3. A 6-story/R3/GM3 first-story brace force versus time.

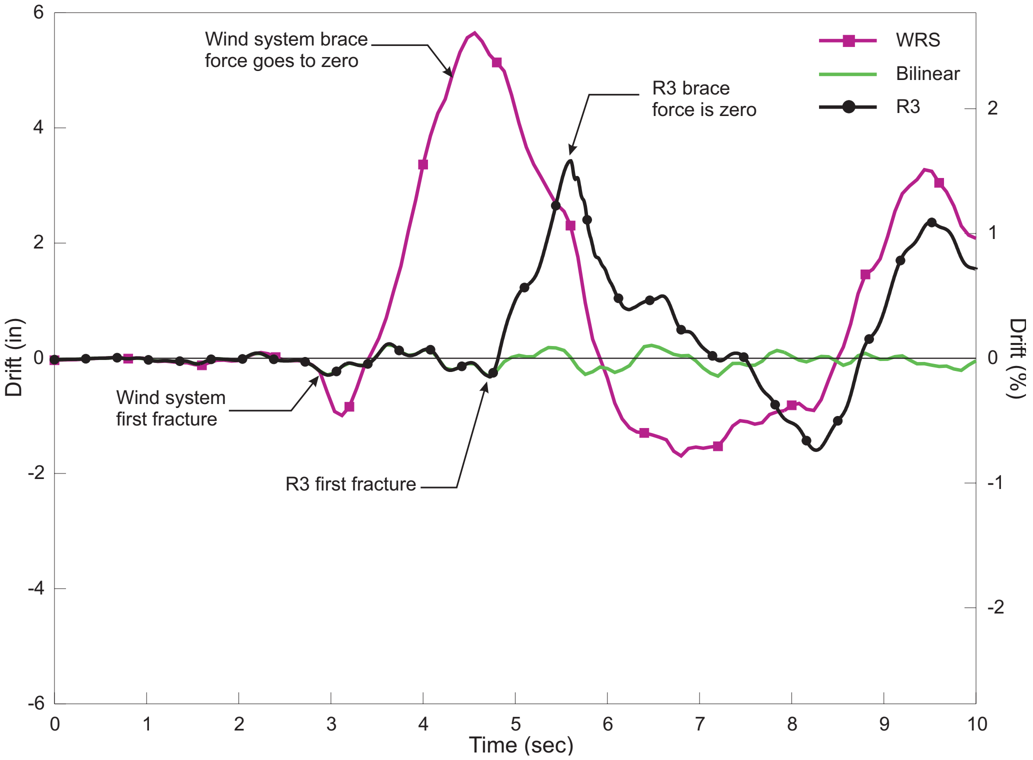

Fig. A-4. A 6-story/R3/GM3 first-story brace displacement.

Table A-2. Ground Motion Records

Earthquake	GM	Record	Magnitude	Distance [km]
Mammoth Lakes	1	ER-A-LVL000	6.0	19.7
	2	ER-A-LVL090		
Tabas	3	ER-FER-L1	7.4	94.4
	4	ER-FER-T1		
Landers	5	ES-H05000	7.3	69.5
	6	ES-H05090		
Kocaeli	7	ER-MCD000	7.4	62.3
	8	ER-MCD090		
San Fernando	9	ES-SJC033	6.6	104
	10	ES-SJC303		
Northridge	11	ER-SOR225	6.7	54.1
	12	ER-SOR315		
Morgan Hill	13	ER-CLS220	6.2	22.7
	14	ER-CLS310		

when viewed as a function of time than as hysteretic behavior. Such a plateau probably protected most models from collapsing under a single pulse by requiring brace forces to reverse before allowing any loss in capacity. Though the plateau is unrealistic, it represents a modeling compromise made for the sake of numerical convergence and should be assessed as slightly unconservative. For further information regarding the design and analysis of these models, see Appel (2008).

Boston Ground Motion Suite

Strong motion records for moderate seismic regions are often too scarce to assemble adequate suites of ground motions for performance assessments. These limited data require either the development of artificial ground motions or the adaptation of records from measured events in higher seismic regions. Furthermore, the lack of data implies that uncertainty related to earthquake magnitude and distance is probably greater in moderate seismic regions than in high seismic regions. For instance, Figure A-5 shows the 1-Hz deaggregation of seismic hazard for Boston and for a location in Los Angeles. The LA hazard appears to derive from only two major sources and a few minor sources, whereas the Boston hazard derives from a multitude of separate sources. This variability in possible earthquake magnitudes is typical for the Eastern North America (ENA) seismic hazard.

The suite of ground motions used in this study was developed such that the average acceleration response spectrum (ARS) curve for 14 motions matched the IBC 2006 MCE for Site Class B. Every motion in the suite was required to match or exceed at least one U.S. Geological Survey (USGS) uniform hazard spectrum (UHS) point at T = 0.0, 0.1, 0.2, 0.3, 0.5, 1.0 or 2.0 seconds without scaling. Table A-2 lists the selected 14 ground motions recorded from seven different earthquake sources. In anticipation of future three-dimensional (3D) simulations, an orthogonal pair of motions was selected from each earthquake. For this two-dimensional (2D) study, all 14 motions were applied independently. Figure A-6 compares the selected suite of 14 unscaled ground motions to the UHS points. The Site Class B ARS values were allowed to be as great as 2.0 times or as small as 0.5 times any of the UHS points. Allowing this variation was thought to capture approximately 90% of the hazard represented by the USGS deaggregations (Sorabella, 2006). The Site Class B motions were amplified using the program Equivalent-linear Earthquake site Response Analysis (Bardet and Ichii, 2000), assuming a typical Boston soil profile (Johnson, 1989; Sorabella, 2006). Figure A-7 compares the ARS of the 14 motions with the average ARS and the IBC 2006 Site Class D MCE. Figure A-7 shows resonance of the soil column at approximately 0.9 second, and significantly lower spectral accelerations for all motions for $T > 2.0$ seconds. For this reason, a 15th motion was created artificially to match the Site Class D MCE as closely as possible. Figure A-8 compares the ARS of the spectral compatible motion, created using the program SIMQKE (Carr, 2004), to the Site Class D MCE as well as the 14 ground motion suite average. See Hines et al. (2009) for further discussion of issues related to the selection of ENA ground motion suites.

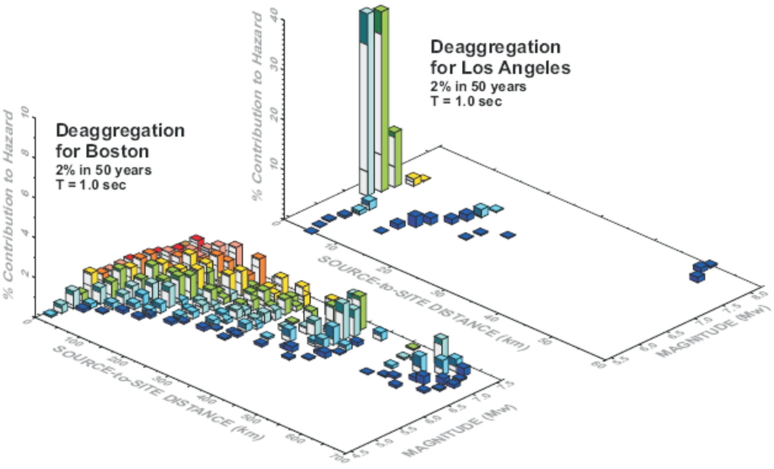

Fig. A-5. A 2% in 50-year (Frankel et al., 2002) deaggregation for Boston and LA at T = 1.0 s. (adapted from files downloaded from http://www.usgs.gov)

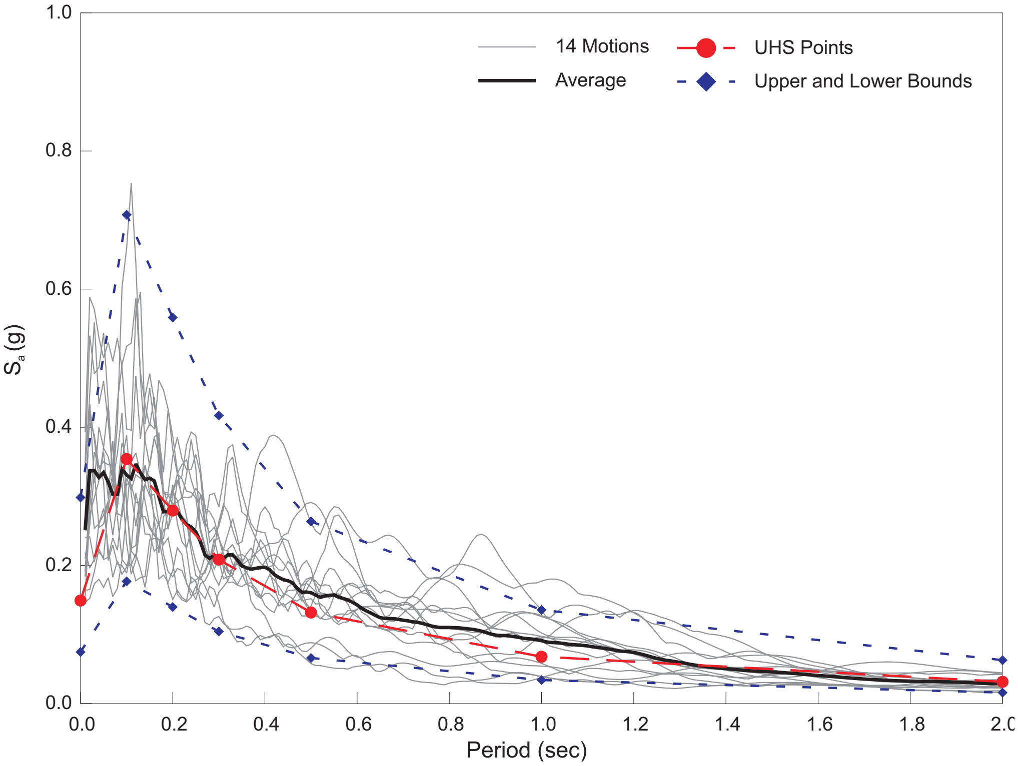

Fig. A-6. Selected 2002 14 ground motion suite—Site Class B.

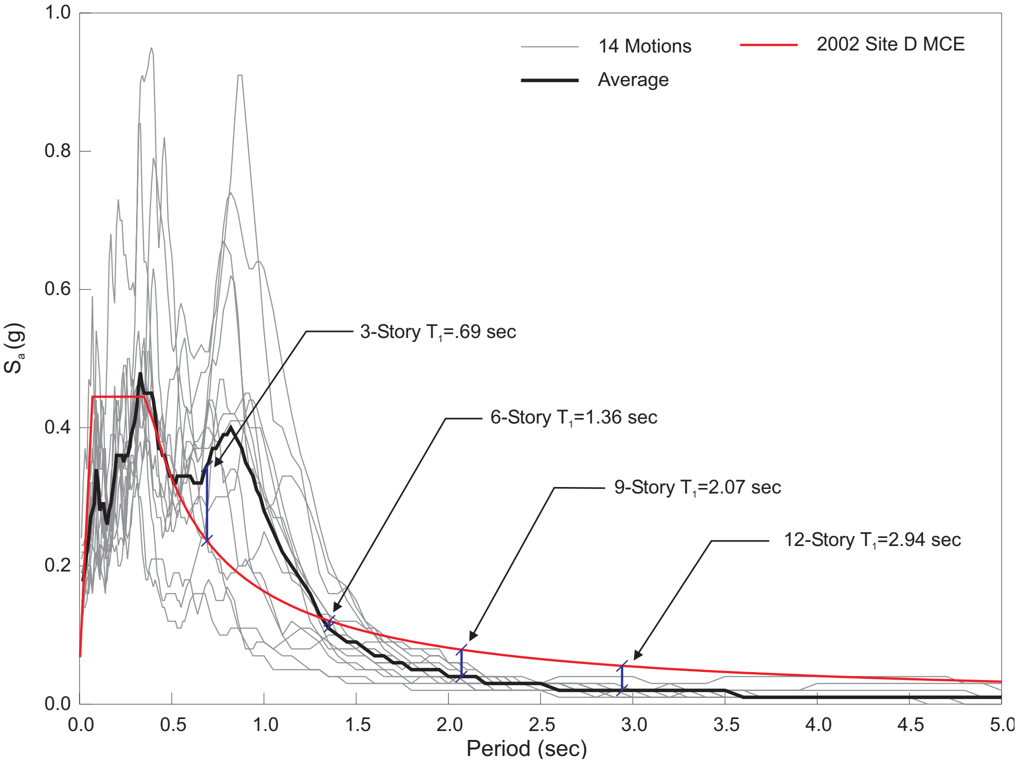

Fig. A-7. The 14 ground motion suite amplified through Site Class D soil column.

Performance Assessment: FEMA-350 versus ATC-63

The methods proposed in FEMA-350 (SAC, 2000a) and ATC-63 (ATC, 2008) differ substantially in their characterization of system demand and capacity and provide very different assessments for particular low-ductility buildings. After introducing the principal difference between these two methods—developed to assess higher ductility systems in high seismic regions—results for this study are presented according to a modified version of the ATC-63 method.

The FEMA-350 approach (SAC, 2000a; Cornell et al., 2002; Yun et al., 2002; Lee and Foutch, 2002) assumes that maximum interstory drift is the best indicator of collapse demand and capacity. This assumption is consistent with the general understanding that nonlinear structural behavior under seismic loads is more accurately assessed according to displacements than according to forces. For the purposes of the FEMA-350 approach, however, interstory drifts were assumed to be linearly related to spectral acceleration (Cornell et al., 2002). The use of displacements as engineering demand parameters (EDPs) to evaluate collapse has recently come under criticism, based on the observation that these EDP demands "become very sensitive to small perturbations when the system is close to collapse" (Ibarra and Krawinkler, 2005, p. 282).

For low-ductility systems, this problem is compounded in the assessment of the drift demand parameter, *D*. Since low-ductility systems either remain elastic or experience significant drift demands once the primary lateral system degrades, the EDP for interstory drift, *D*, can exhibit values that vary by an order of magnitude between ground motions. This wide variation results in a demand randomness factor, γ_r, that is commonly 2 or higher, leading to very low confidence in collapse capacity. Ironically, the confidence can be increased for a given assessment simply by removing the lowest drift demands from the assessment. This is illustrated by an example for the 9-story/R3 model.

The maximum interstory drift demands and capacities are given in Table A-3, for the 9-story/R3 model and the resulting demand and capacity factors reflecting randomness, based on the logarithmic standard deviations, β, of these values are listed in Table A-4. For the purposes of this example, the β values for uncertainty are assumed to be 0.400, reflecting an increased level of uncertainty associated with the analysis of low-ductility braced frame systems when compared to the moment frame systems for which the procedure was originally calibrated.

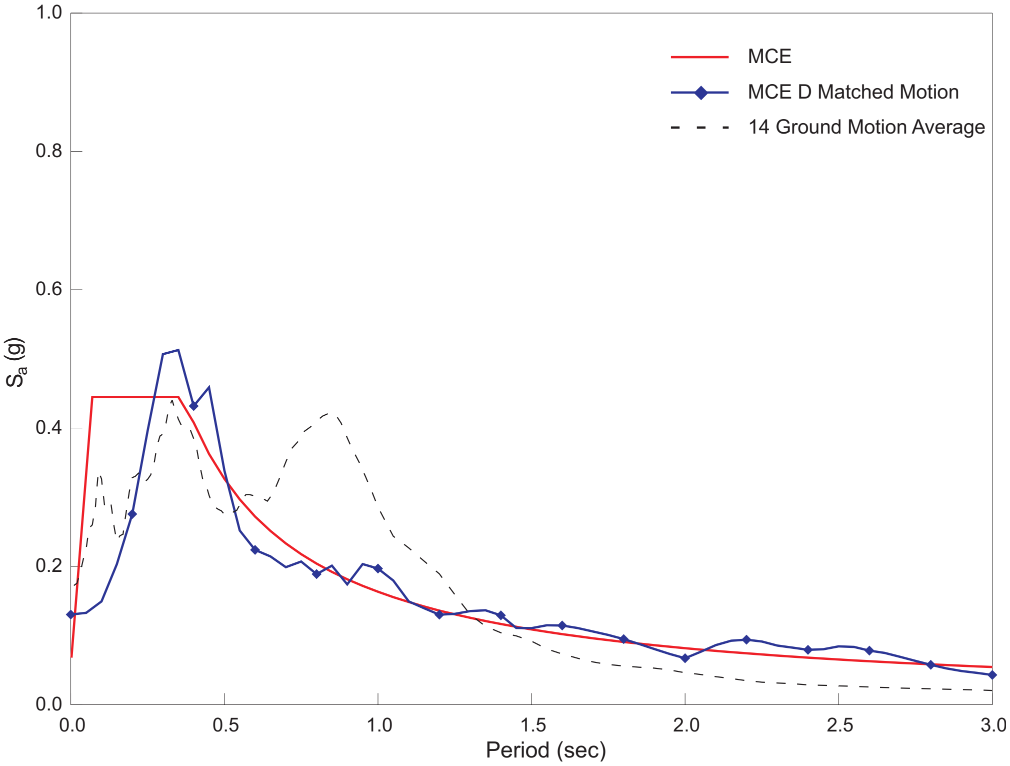

Fig. A-8. Matched motion ARS comparison.

Table A-3. Maximum Interstory Drift Demands and Capacities for 15 Ground Motions

Motion	Demand	Capacity
GM1	0.018	0.033
GM2	0.003	0.040
GM3	0.014	0.022
GM4	0.015	0.028
GM5	0.021	0.050
GM6	0.029	0.022
GM7	0.002	0.039
GM8	0.003	0.018
GM9	0.016	0.038
GM10	0.003	0.017
GM11	0.020	0.019
GM12	0.012	0.018
GM13	0.024	0.031
GM14	0.027	0.025
Matched	0.024	0.030
Median	**0.0160**	**0.0283**

Combination of these values results in

$$\lambda = \frac{\gamma_R \gamma_U D}{\varphi_R \varphi_U C} = \frac{(1.85)(1.12)(0.0160)}{(0.918)(0.890)(0.0283)} = 1.43 \qquad (1)$$

where

γ_R = demand variability factor
γ_U = analysis uncertainty factor
D = median maximum drift demand for the unscaled motion
φ_R = resistance factor accounting for random behavior
φ_U = resistance factor accounting for uncertainty in analytic modeling
C = median maximum drift capacity according to IDAs

which yields $K_x = -0.22$ and a confidence of 41%.

Note, however, that GM2, 7, 8 and 10 produced demand drifts measuring in tenths of a percent, while the remaining ten motions produced demand drifts over 1% (Table A-3). Such low drift demands reflect the tendency of the system to perform in the elastic range under these ground motions at a scale factor (SF) of 1.0. Since Table A-3 reports only four such instances, the median demand, $D = 0.0160$, is still in the higher range of values. Equation 1 shows that $\gamma_R = 1.85$ has the most significant effect on confidence level. If these four motions are removed from the assessment, the median demand increases, but not enough to offset the increase in confidence. Combination of these values results in a confidence of 65%. (See Tables A-5 and A-6 pn page 175).

Table A-4. Demand and Capacity Factors per FEMA-350 Assessment for 15 Ground Motions

Demand		Capacity	
β_{DR}	0.916	β_{CR}	0.343
γ_R	1.85	φ_R	0.918
β_{DU}	0.400	β_{CU}	0.400
γ_U	1.12	φ_U	0.890

The addition of more ground motions to the suite would probably not result in greater accuracy if the distribution continues to bifurcate between elastic and inelastic behavior, as shown in Figure 6. Such behavior distinguishes low-ductility braced frame systems from their higher ductility counterparts, whose transition into the inelastic range is generally expected to be smoother. If, for some reason, the median demand value fell into the elastic range, the resulting confidence would be unconservatively high. It could be argued that the effects of this bifurcation on the FEMA-350 approach could be mitigated by scaling the ground motions to the code spectral value at the first natural period, S_{aT1}, as recommended. The ATC-63 approach, however, demonstrated little sensitivity to the wide variety allowed within the suite and was therefore better suited to incorporate uncertainty related to earthquake intensity.

In addition to the sensitivity mentioned by Ibarra and Krawinkler (2005), this drift demand sensitivity motivates the assessment of collapse capacity according to earthquake intensity rather than drift demand and capacity. Since the models and incremental dynamic analyses used to assess collapse earthquake intensity are the same used for assessing interstory drifts, there is no danger in abandoning the “displacement-based” FEMA-350 approach in favor of an intensity-based parameter. Sensitivity to displacement behavior is preserved in the IDAs. Figure 6 shows the IDA curves for the 9-story/R3 model and demonstrates that variation in behavior can be observed either in terms of drift, or in terms of ground motion intensity. The IDA curve for GM4 shows that the model stayed in the elastic range until SF = 1.7 and just before collapse. Compare this result to the curve for GM11, where at SF = 1.0. The model already experienced inelastic behavior; however, it did not collapse until SF = 2.2. Note that almost every IDA curve exhibits a plateau between elastic and inelastic behavior, where the transition is made from primary LFRS to reserve LFRS.

Since drift demands appear bifurcated rather than lognormally distributed for the low-ductility LFRS in question, and since ground motion intensity, expressed in spectral acceleration, S_a, or SF gives at least as good an indication of

Table A-5. Maximum Interstory Drift Demands and Capacities for 11 Ground Motions

Motion	Demand	Capacity
GM1	0.018	0.033
GM3	0.014	0.022
GM4	0.015	0.028
GM5	0.021	0.050
GM6	0.029	0.022
GM9	0.016	0.038
GM11	0.020	0.019
GM12	0.012	0.018
GM13	0.024	0.031
GM14	0.027	0.025
Matched	0.024	0.030
Median	**0.0200**	**0.0283**

Table A-6. Demand and Capacity Factors per FEMA-350 Assessment for 11 Ground Motions

Demand		Capacity	
β_{DR}	0.288	β_{CR}	0.312
γ_R	1.06	φ_R	0.931
β_{DU}	0.400	β_{CU}	0.400
γ_U	1.12	φ_U	0.890

variability in collapse capacity as interstory drift, it is attractive to use an approach more similar to ATC-63. This approach focuses on spectral acceleration as an intensity measure and avoids discussing drift demands all together. IDA results are represented in the form of cumulative distribution functions, or fragility curves. These fragility curves provide not only a numerical indication but also visual indication of a particular system's resistance to collapse (see Figures 11 through 14).

Figure A-9 shows fragility curves for the 9-story/R3 and WRS models in terms of S_{a1}, with a collapse probability for the R3 model of close to 70%. In this figure, the smooth fragility curve is a cumulative distribution function based on the median and lognormal standard deviation of the experimental data points. The high probability of collapse reflects a characteristic of the ground motion suite that may provide further reason to differentiate the assessment of low-ductility systems in moderate seismic regions from high ductility systems in high seismic regions. Figure A-7 shows that the

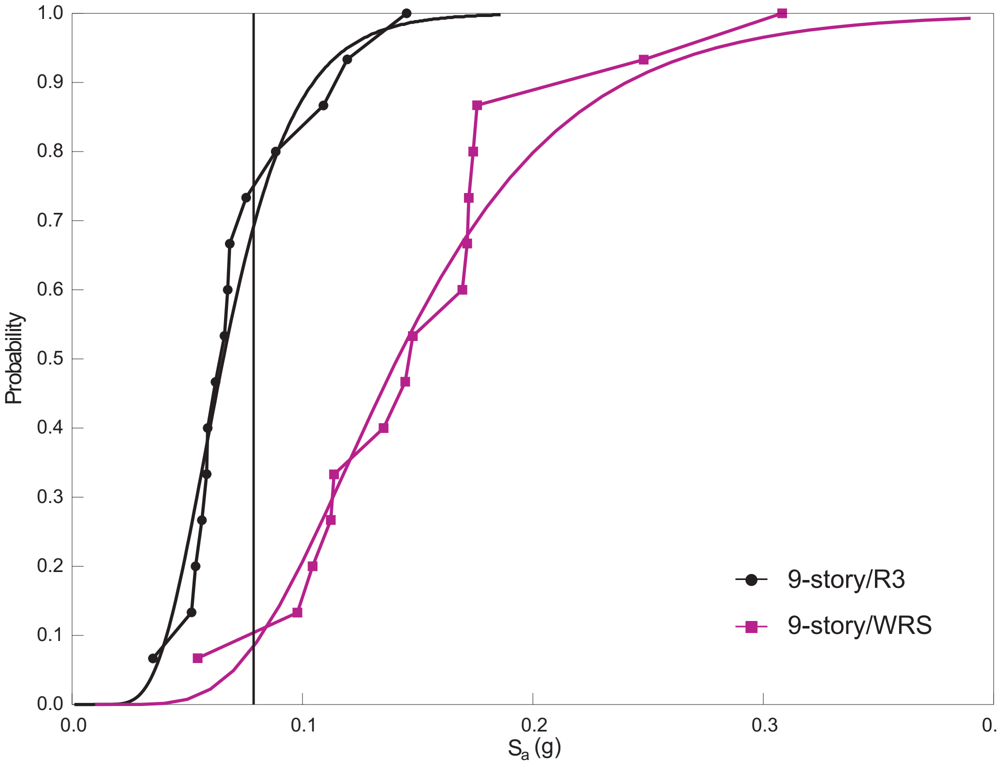

Fig. A-9. The 9-story/R3 and WRS fragility curves as a function of S_a.

average S_{a1} (T_1 = 2.07 seconds) value for the suite falls well below the MCE value given by IBC 2006 for Site Class D. These low spectral accelerations in the first mode are considered to be more realistic and more consistent with the state of the art related to ENA ground motions than the IBC 2006 curve (Sorabella, 2006; Hines et al., 2009). This phenomenon, combined with the presence of higher mode effects due to ARS spikes at lower periods suggests that evaluating fragility based on SF rather than S_a may be more realistic for low-ductility systems in moderate seismic regions. Using SF is similar to using S_{aT1} for the suite average rather than for the IBC MCE. Note that the IDAs in this assessment did not account for the fact that less soil amplification would be expected for larger motions due to nonlinear soil behavior. In order to take this into account, it would perhaps be more accurate to increment the rock motion and reevaluate the nonlinear soil column analysis at each increment. Such a procedure is beyond the scope of the present work. For now, it can be assumed that this part of the assessment is conservative since it does not take into account decreasing soil amplification with increasing intensity of bedrock ground motions. Figure A-10 shows the 9-story/R3 fragility curve in terms of SF, which is normalized to 1 for the original Site Class D suite.

The fragility curves in Figure A-9 express implicitly another characteristic of the suite used for this assessment. As discussed previously, no rock motions were scaled prior to their inclusion in the suite so as to allow maximum realistic variation in ground motion characteristics. Based on this suite, there is legitimate concern that the fragility curves merely reflect the level of variation allowed in choosing the rock motions. If this were the case, then the smallest motions would have the largest scale factors and the largest motions would have the smallest scale factors. In order to address this concern, Figure A-10 also shows normalized S_a values for each motion and for each of the first three modes ordered in the same manner as the values composing the fragility curves. S_a values were normalized for each mode by dividing the S_a for that mode (first, second or third) and ground motion (GM 1-14 or "Matched) by the S_a value for the same mode as defined by the IBC 2006 MCE ARS curve. Strict correlation with variations in rock motion intensity would imply a negative slope to each of the normalized S_a curves. While some general negative slope can be discerned for each set of S_a values, it is overwhelmed by variations in the normalized S_a values themselves. This demonstrates that higher mode effects and record-to-record (RTR) variability without respect to variations in *M-R* values provide for substantial variation in the collapse scale factors between ground motions. Similar variations in second and third mode normalized S_a values can be observed in Figure A-11 for the 9-story/WRS model.

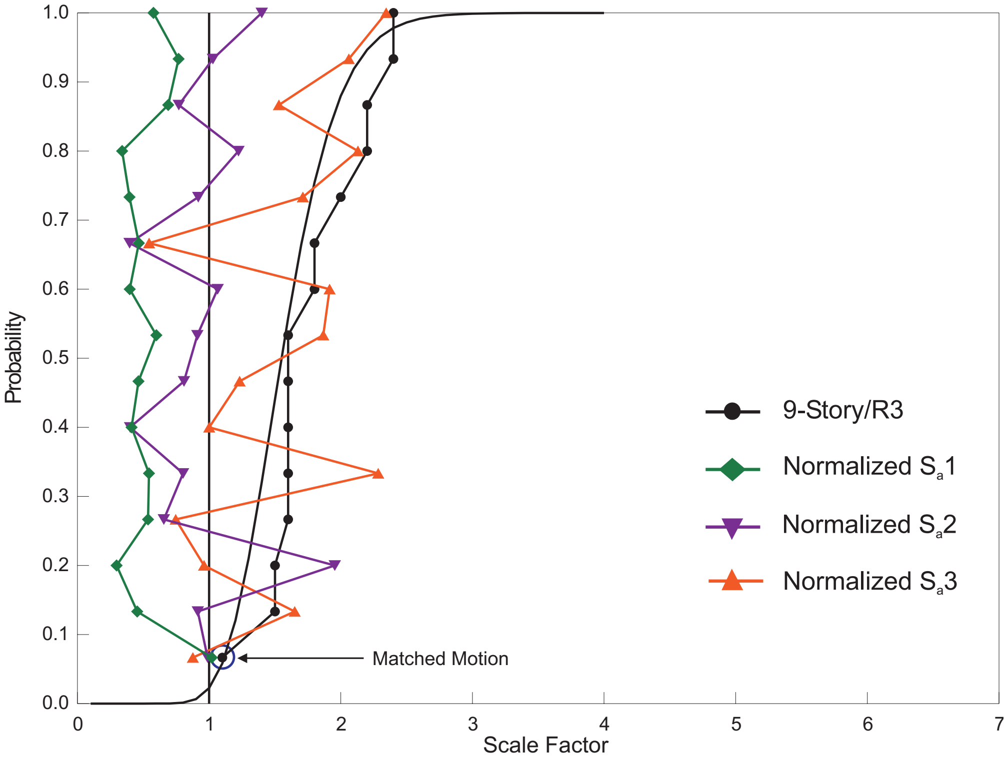

Fig. A-10. The 9-story/R3 fragility curve as a function of SF.

Figure A-10 and Figure A-11 reinforce the observation from Figure A-9 that the WRS design improved collapse resistance significantly beyond the R3 design. Figures 11 through 14 depict final fragility curves for each model as lognormal distributions based on the median scale factors from the suite of 15 motions and a uniform standard deviation of

$$\beta_{TOT} = \sqrt{\beta^2_{RTR} + \beta^2_{DR} + \beta^2_{TD} + \beta^2_{MDL}} \qquad (2)$$

$$= \sqrt{0.4^2 + 0.4^2 + 0.4^2 + 0.4^2} = 0.8$$

where

β_{TOT} = total system collapse uncertainty
β_{RTR} = record-to-record collapse uncertainty
β_{DR} = design requirements-related collapse uncertainty
β_{TD} = test data-related collapse uncertainty
β_{MDL} = modeling-related collapse uncertainty

These values are recommended by Chapters 5 and 7 of ATC-63 for an assessment considered to be "good." For comparison to the ATC-63 values, Table A-7 lists β_{RTR} values calculated from the 15 analysis cases for each model, and the resulting β_{TOT} value. β_{RTR} = 0.40 was used in lieu of the values reported in Table A-7 for three reasons: consistency with ATC-63, similarity between the calculated β_{RTR} values and the ATC-63 recommended value, and the ATC-63 value derives from a significantly greater number of analysis cases. It may be appropriate to modify the ATC-63 β_{RTR} value for low-ductility systems in moderate seismic regions; however, such a decision should be based on more than 15 ground motions.

Table A-7. Calculated β_{RTR} Values

	β	R2	R3	R4	WRS
3 Story	RTR	0.365	0.385	0.385	0.286
	Total	0.790	0.799	0.799	0.756
6 Story	RTR	0.447	0.447	0.354	0.390
	Total	0.830	0.830	0.785	0.802
9 Story	RTR	0.383	0.212	0.314	0.463
	Total	0.798	0.731	0.767	0.839
12 Story	RTR	0.411	0.386	—	0.389
	Total	0.812	0.740	—	0.801

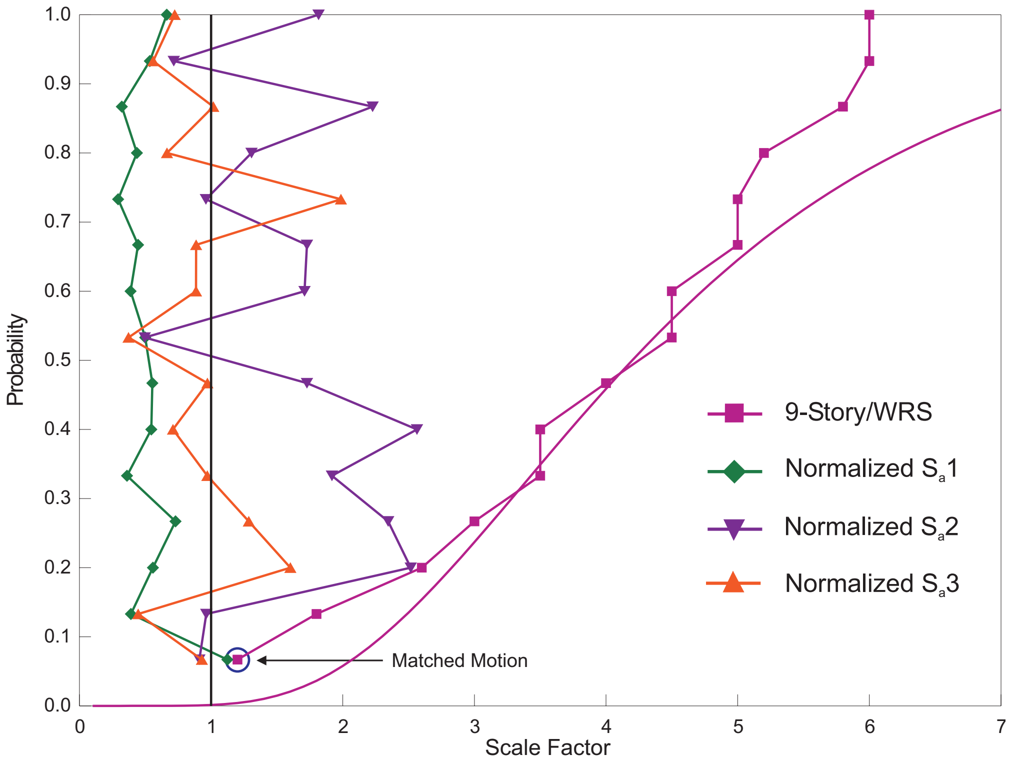

Fig. A-11. The 9-story/WRS fragility curve as a function of SF.

ABBREVIATIONS

ARS	acceleration response spectrum
ASD	Allowable Strength Design
ATC	Applied Technology Council
CBF	concentric braced frame
CUREE	Consortium of Universities for Research in Earthquake Engineering
EDP	engineering demand parameter
ENA	Eastern North America
FEMA	Federal Emergency Management Agency
GM	ground motion
HSS	hollow structural section
LFRS	lateral force resisting system
LRFD	Load Resistance Factor Design
IDA	incremental dynamic analysis
M-R	magnitude-distance
MCE	maximum considered earthquake
OCBF	ordinary concentric braced frame
OMRF	ordinary moment resisting frame
RTR	record-to-record (variability)
SAC	SEAOC-ATC-CUREE
SDC	Seismic Design Category
SEAOC	Structural Engineering Association of California
SF	scale factor
UHS	uniform hazard spectrum
WRS	wind plus reserve system

SYMBOLS

A_g = section gross area

b/t = width/thickness

C = median maximum drift capacity from IDAs

D = median maximum drift demand from IDAs

F_y = yield stress

K = effective length factor

K_x = Gaussian variate

M_p = plastic moment capacity

R = response modification factor

Ry = ratio of expected yield stress to specified minimum yield stress

S_a = spectral acceleration

S_{aT1} = spectral acceleration at the first natural period of a structure

W = building seismic weight

β (beta) = logarithmic standard deviation

β_{CR} = beta for aleatory uncertainty associated with structure capacity (FEMA-350)

β_{CU} = beta for epistemic uncertainty associated with structure capacity (FEMA-350)

β_{DR} = beta for aleatory uncertainty associated with structure demand (FEMA-350)

β_{DR} = beta for design requirements related to collapse uncertainty (ATC-63)

β_{DU} = beta for epistemic uncertainty associated with structure demand (FEMA-350)

β_{RTR} = beta for record-to-record variability (ATC-63)

β_{MDL} = beta for modeling uncertainty (ATC-63)

β_{TD} = beta for uncertainty related to test data (ATC-63)

β_{TOT} = beta for total system collapse uncertainty (ATC-63)

γ_r = demand variability factor (FEMA-350)

γ_u = analysis uncertainty factor (FEMA-350)

ϕ_r = resistance factor accounting for random (aleatory) behavior (FEMA-350)

ϕ_u = resistance factor accounting for uncertainty in analytical modeling

Ω = system overstrength factor

REFERENCES

AISC (1992), *Seismic Provisions for Structural Steel Buildings*, American Institute of Steel Construction, Inc., Chicago.

AISC (1997a), *Seismic Provisions for Structural Steel Buildings*, American Institute of Steel Construction, Inc., Chicago.

AISC (1997b), *Hollow Structural Sections, Connections Manual*, American Institute of Steel Construction, Inc., Chicago.

AISC (2002), *Seismic Provisions for Structural Steel Buildings*, ANSI/AISC 341-02, American Institute of Steel Construction, Inc., Chicago, May 21.

AISC (2005a), *Specification for Structural Steel Buildings*, ANSI/AISC 360-05, American Institute of Steel Construction, Inc., Chicago, March 9.

AISC (2005b), *Seismic Provisions for Structural Steel Buildings*, ANSI/AISC 341-05, American Institute of Steel Construction, Inc., Chicago, March 9, with Supplement No. 1, November 15.

Anderson, J.C. (1975), "Seismic behavior of K-Braced Frames," *Journal of the Structural Division*, ASCE, Vol. 101, No. 10.

Appel, M.E. (2008), *Design and Performance of Low-Ductility Chevron Braced Frames under Moderate Seismic Demands*, Masters Thesis, Department of Civil and Environmental Engineering, Tufts University, Medford, MA.

ASCE (2005), *Minimum Design Loads for Buildings and Other Structures*, ASCE/SEI 7-05, American Society of Civil Engineers, Reston, VA.

ATC (1978), *Tentative Provisions for the Development of Seismic Regulations for Buildings*, ATC-3-06, Applied Technology Council, NBS Special Publication 510, NSF Publication 78-8, U.S. Government Printing Office, Washington, D.C.

ATC (2008), Quantification of Building Seismic Performance Factors, ATC-63 Project Report—90% Draft, FEMA P695, Applied Technology Council, Redwood City, CA, April.

Bardet, J.P., Ichii, K. and Lin, C.H. (2000), *A Computer Program for Equivalent-Linear Earthquake Site Response Analyses of Layered Soil Deposits*, Department of Civil Engineering, University of Southern California, August, 40 pp.

Bell, G.R. and Lamontagne, A.S. (2002), "Use of Total Hazard in Examining Seismic Risk Considerations in Building Design," *EERI 7th National Conference on Earthquake Engineering*, Boston, July 21–25.

Bruneau, M., Tremblay, R., Timler, P. and Filliatrault, A. (1995), "Performance of Steel Structures during the 1994 Northridge Earthquake," *Canadian Journal of Civil Engineering*, Vol. 22, pp. 338–360.

Carr, A.J. (2004), *Ruaumoko Manual Volumes 1 & 2*, University of Canterbury, Christchurch, New Zealand, 333 pp.

Cornell, C.A, Jalayer, F., Hamburger, R.O. and Foutch, D.A. (2002), "Probabilistic Basis for 2000 SAC Federal Emergency Management Agency Steel Moment Frame Guidelines," *Journal of Structural Engineering*, ASCE, April, pp. 526–533.

Engelhardt. M.D. and Popov, E.P. (1989), Behavior of Long Links in Eccentrically Braced Frames, UCB/EERC-89/01, Earthquake Engineering Research Center, University of California at Berkeley, Richmond, CA.

EQE International (1997), Second Pilot Test Study of the Standardized Nationally Applicable Loss Estimation Methodology, Boston, Massachusetts, Final Report, Prepared for the National Institute of Building Sciences, March.

Frankel, A., Petersen, M.D., Mueller, C., Haller, K.M., Wheeler, R.L., Leyendecker, E.V., Wesson, R.L., Harmsen, S.C., Cramer, C.H., Perkins, D.M. and Rukstales, K.S. (2002), Documentation for the 2002 Update of the National Seismic Hazard Maps, United States Geological Survey, Open-File Report 02-420, Denver.

Gryniuk, M.C. and Hines, E.M. (2004), Safety and Cost Evaluation of a Steel Concentrically Braced Frame Student Residence Facility in the Northeastern United States, Preliminary Report to the American Institute of Steel Construction, LeMessurier Consultants, Cambridge, MA, December.

Hines, E.M and Appel, M.E. (2007), "Behavior and Design of Low-Ductility Braced Frames," *ASCE Structures Congress*, Long Beach, CA, May.

Hines, E.M., Sorabella, S. and Baise, L.G. (in review 2009), "Ground Motion Suite Selection for Eastern North America," *Journal of Structural Engineering,* ASCE.

ICC (2006), *International Building Code*, International Code Council, Falls Church, VA.

Ibarra, L. and Krawinkler, H (2005), Global Collapse of Frame Structures under Seismic Excitation, Blume Center Technical Report No. 152, Stanford University, Palo Alto, CA, August, 349 pp.

Johnson, E.J. (1989), "Geotechnical Characteristics of the Boston Area," *Civil Engineering Practice*, Boston Society of Civil Engineers Section/ASCE, Vol. 4, pp. 53–64.

Kim, J. and Choi, H. (2004), "Response Modification Factors of Chevron-Braced Frames," *Engineering Structures*, Vol. 27, pp. 285–300.

Khatib, I.F., Mahin, S.A. and Pister, K.S. (1988), Seismic Behavior of Concentrically Braced Steel Frames, UCB/EERC Report 88/01, Earthquake Engineering Research Center, University of California, Berkeley, Richmond, CA, January.

Lee, K. and Foutch, D.A (2002), "Seismic Performance Evaluation of Pre-Northridge Steel Frame Buildings with Brittle Connections," *Journal of Structural Engineering*, ASCE, Vol. 28, No. 4, April, pp. 546–555.

Leyendecker, E.V., Hunt, R.J, Frankel, A.D and Rukstales, K.S (2000), "Development of Maximum Considered Earthquake Ground Motion Maps," *Earthquake Spectra*, Vol. 16, No. 1, February, pp. 21–40.

Liu, J. and Astaneh-Asl (2000), "Cyclic Testing of Simple Connections Including Effects of Slab," *Journal of Structural Engineering*, ASCE, Vol. 126, No. 1, pp. 32–39.

Luft, R.W. and Simpson, H. (1979), "Massachusetts Earthquake Design Requirements," *ASCE Convention and Exposition*, Boston, Preprint 3567, April 2–6.

Massachusetts (1996), *The Massachusetts State Building Code: 780 CMR Sixth Edition.* Massachusetts State Board of Building Regulations and Standards, Boston.

Matsushima, Y. (1969), "Discussion of Restoring Force Characteristics of Buildings, the Damage from Tokachi-oki Earthquake" Report, Annual Meeting, Architectural Institute of Japan, August, pp. 587–588 (in Japanese).

Nakashima, M. and Wakabayashi, M. (1992), "Analysis and Design of Steel Braces and Braced Frames in Building Structures," in *Stability and Ductility of Steel Structures under Cyclic Loading*, Fukumoto, Y. and Lee, G.C. editors, CRC Press, Boca Raton, FL, pp. 309–321.

Nelson, T.A. (2007), "Performance of a 9-Story Low-Ductility Moment Resisting Frame under Moderate Seismic Demands," Masters Thesis, Department of Civil and Environmental Engineering, Tufts University, Medford, Massachusetts.

Rojahn, C. (1995), Structural Response Modification Factors, ATC-19, Applied Technology Council, Redwood City, CA.

SAC (2000a), Recommended Seismic Design Criteria for New Steel Moment-Frame Buildings, FEMA-350, Federal Emergency Management Agency, Washington, D.C.

SAC (2000b), State of the Art Report on Systems Performance of Steel Moment Frames Subject to Earthquake Ground Shaking, FEMA 355C, Federal Emergency Management Agency, Washington, D.C.

SEAOC (1960), Recommended Lateral Force Requirements and Commentary, Seismology Committee, Structural Engineers Association of California, San Francisco.

SEAOC (1974), Recommended Lateral Force Requirements and Commentary, Seismology Committee, Structural Engineers Association of California, San Francisco.

SEAONC (1982), Earthquake Resistant Design of Concentric and K-Braced Frames, Structural Engineers Association of Northern California, Research Committee, July.

Shibata, M. and Wakabayashi, M. (1983a), "Ultimate Strength of K-Type Braced Frame," *Transactions of the Architectural Institute of Japan*, No. 326, pp. 1–9, (in Japanese).

Shibata, M. and Wakabayashi, M. (1983b), "Experimental Study on the Hysteretic Behavior of K-Type Braced Frame Subjected to Repeated Load," *Transactions of the Architectural Institute of Japan*, No. 326, pp. 10–16 (in Japanese).

Sorabella, S. (2006), *Ground Motion Selection for Boston, Massachusetts*, Masters Thesis, Department of Civil and Environmental Engineering, Tufts University, Medford, Massachusetts.

Tremblay, R. (2001), "Seismic Behavior and Design of Concentrically Braced Steel Frames," *Engineering Journal*, AISC, Vol. 38, No. 3, 3rd Quarter, pp. 148–166.

Tremblay, R., Bruneau, M., Nakashima, M., Prion, G.L., Filliatrault, A. and DeVall, R. (1996), "Seismic Design of Steel Buildings: Lessons from the 1995 Hyogo-ken Nanbu Earthquake," *Canadian Journal of Civil Engineering*, Vol. 23, pp. 727–756.

Tremblay, R. and Robert, N. (2000), "Seismic Design of Low- and Medium-Rise Chevron Braced Steel Frames," *Canadian Journal of Civil Engineering*, Vol. 27, pp. 1192–1206.

Tremblay, R. and Robert, N. (2001), "Seismic Performance of Low- and Medium-Rise Chevron Braced Steel Frames," *Canadian Journal of Civil Engineering*, Vol. 28, pp. 699–714.

Uang, C.M. and Bertero, V. (1986), Earthquake Simulation Tests and Associated Studies of a 0.3-Scale Model of a Six-Story Concentrically Braced Steel Structure, UCB/EERC-86/10, Earthquake Engineering Research Center, University of California at Berkeley, Richmond, CA, December.

Vamvatsikos, D. and Cornell, C.A. (2002), "Incremental Dynamic Analysis," *Earthquake Engineering and Structural Dynamics*, 31, pp. 491–514.

Yanev, P.I., Gillengerten, J.D., and Hamburger, R.O. (1991), *The Performance of Steel Buildings in Past Earthquakes.* American Iron and Steel Institute and EQE Engineering, Inc.

Yun, S.Y., Hamburger, R.O., Cornell, C.A., and Foutch, D. (2002), "Seismic Performance Evaluation of Steel Moment Frames, *Journal of Structural Engineering*, ASCE, Vol. 128, No. 4, April, pp. 534–545.